DHBW
Duale Hochschule
Baden-Württemberg
Ravensburg

Duale Hochschule Baden-Württemberg · Ravensburg
Fallenbrunnen 2, 88045 Friedrichshafen

Prof. Dr.-Ing. Markus Grieb
Lehrprofessor für Luft- und Raumfahrtsysteme

DHBW Ravensburg
Campus Friedrichshafen
Fallenbrunnen 2
88045 Friedrichshafen

Telefon + 49 . 7541 . 2077 - 452
Telefax + 49 . 7541 . 2077 - 198

grieb@dhbw-ravensburg.de
www.technik.dhbw-ravensburg.de

11.07.2023

Eigenständigkeitserklärung

Sehr geehrte Damen und Herren,

hiermit bestätige ich, dass die teilnehmenden Studierenden mit dem Thema:

DLR Challenge 2023

selbstständig verfasst und keine anderen als die angegebenen Quellen und Hilfsmittel benutzt haben

Friedrichshafen, den 11.07.2023

Mit freundlichen Grüßen

Prof. Dr.-Ing. Markus Grieb

DHBW Ravensburg
Campus Ravensburg
Marienplatz 2
88212 Ravensburg

Telefon + 49 . 751 . 18999 - 2700
Telefax + 49 . 751 . 18999 - 2701

DHBW Ravensburg
Campus Friedrichshafen
Fallenbrunnen 2
88045 Friedrichshafen

Telefon + 49 . 7541 . 2077 - 0
Telefax + 49 . 7541 . 2077 - 199

info@dhbw-ravensburg.de
www.dhbw-ravensburg.de

THE *SENTINEL* SYSTEM

Lara Obert, Erwin Aust, Lukas Deuschle, Niels Marr, Luca Stoll, Edgar Kirchner
Luft-und Raumfahrttechnik, Bachelorstudiengang 4. Semester
Duale Hochschule Baden-Württemberg
Betreuung: Prof. Markus Grieb

Abstract

This paper is part of the 2023 DLR challenge, which states the task of designing an aircraft which will replace collapsed communication pathways after a disaster. The following draft presents the process and final result of an aircraft system suitable for the above mentioned task. The conceptual phase is described in detail, explaining the simulation and discussion of different concepts and ideas. Custom simulation approaches and algorithms are derived and explained. Having selected a preliminary design, the airframe geometry was designed and brought to life in CAD. The aerodynamic properties of the aircraft were tested via CFD simulations. Apart from the structural design, the weather conditions have been researched, the logisitics of the ground segment were planned and all required subsystems were researched and designed adequately for mission. A thermal analysis of the aircraft was conducted, confirming the concept. The final result is presented and described in detail.

Zusammenfassung

Das folgende Paper ist Teil der DLR Challenge 2023, welche die Aufgabe stellt, ein Flugzeug zu entwerfen, das nach einer Katastrophe zusammengebrochene Kommunikationswege ersetzen soll. Der folgende Entwurf präsentiert den Prozess und das endgültige Ergebnis eines Flugzeugsystems, welches das präsentierte Problem löst. Die konzeptionelle Phase wird detailliert beschrieben und erläutert die Simulation und Diskussion verschiedener Ansätze und Ideen. Individuelle Simulationskonzepte und Algorithmen werden abgeleitet und erklärt. Nach Auswahl eines vorläufigen Designs wurde die Geometrie des Flugzeugrumpfes entworfen und in CAD zum Leben erweckt. Die aerodynamischen Eigenschaften des Flugzeugs wurden mittels CFD-Simulationen getestet. Neben dem strukturellen Design wurden die Wetterbedingungen erforscht, die Logistik des Bodensegments wurde geplant und alle erforderlichen Subsysteme wurden angemessen für die Mission untersucht und entworfen. Eine thermische Analyse des Flugzeugs wurde durchgeführt, um die Tauglichkeit des Konzept zu bestätigen. Das endgültige Ergebnis wird detailliert dargestellt und beschrieben.

Keywords
DLR Challenge, Sentinel System, DHBW, Communication

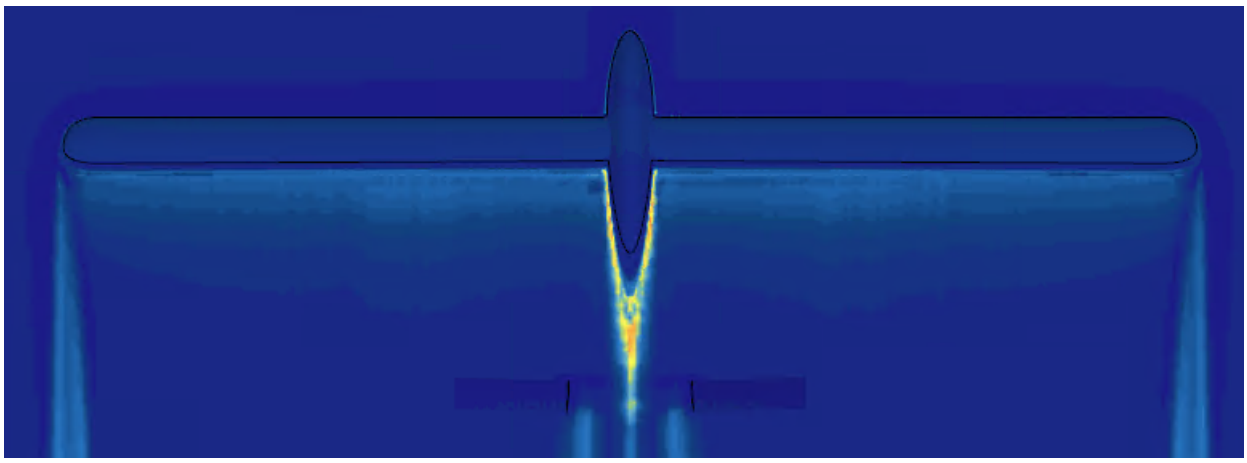

Table of contents

NOMENCLATURE

F_{thrust}	Thrust	N
J	Level of progress	
M_thrust	Torque	$N \cdot m$
R	Radius of the earth	m
Re	Reynolds Number	
S	Reference wing area	m^2
T_a	Atmospheric temperature	K
T_f	Equilibrium fuselage temperature	K
V_{cruise}	cruising speed TAS	$\frac{m}{s}$
$V_{landing}$	Landing speed TAS	$\frac{m}{s}$
V_{max}	Maximum speed TAS	$\frac{m}{s}$
$V_{takeoff}$	Takeoff speed TAS	$\frac{m}{s}$
α	Coefficient of heat transfer	$\frac{W}{m^2 \cdot K}$
α_0	Zero lift angle of attack	
δ	Boundary layer thickness	m
$\dot{Q}$	Heat flow	W
η_f	Engine power to fuselage	
λ	Thermal conductivity	$\frac{W}{m \cdot K}$
ϕ_f	Gravimetric energy density	$\frac{J}{Kg}$
$\rho(h)$	Density	$\frac{Kg}{m^3}$
ρ_{0m}	Density at 0m	$\frac{Kg}{m^3}$
ρ_{18000m}	Density at 18000m	$\frac{Kg}{m^3}$
$\vec{K}$	Position vector	m
$\vec{P}$	Position of radar	m
$\vec{R}$	Radar vector	m
$\vec{S}$	State vector	
$\vec{a}$	Acceleration vector	$\frac{m}{s^2}$
c_f	Thrust coefficient	
c_m	Torque coefficient	
c_{A_α}	Lift coefficient	
c_{w_0}	Zero lift coefficient	
c_{w_α}	Drag coefficient as a function of α	
c_{w_i}	Induced drag coefficient	
d	Great-circle distance	m
g	Gravitational acceleration	$\frac{m}{s^2}$
h	Altitude	m
h	Radar tower height	m
l_m	mean chord	m
$m_{cruise/max}$	mass with half full tank	Kg
m_e	Empty mass	Kg
m_{fuel}	Fuel mass	Kg
$m_{landing}$	mass with empty tank	Kg
m_{tow}	Maximum take off weight	Kg
m_{ttow}	Maximum take off weight	Kg
m_{struct}	Structural mass	Kg
m_{tot}	Total mass	Kg
n_{lim}	Limit load factor	
n_{ult}	Ultimate load factor	
t	Layer thickness	m
x, y, z	3D positions	m
ARF	Aircraft reference frame	
CoM	Center of Mass	
DEFC	Direct Ethanol Fuel Cell	
DLR	Deutsches Zentrum für Luft-und Raumfahrt	
DMFC	Direct Methanol Fuel Cell	
ESRF	Earth surface reference frame	
FOV	Field of View	
GDP	General Design Principle	
LNG	Liquefied natural gas	
LoS	Line of Sight	
LPG	Liquefied petrol gas	
MTOW	Maximum Take off weight	
TAS	True air speed	

1. DESIGN OVERVIEW

Requirements	
Rapid reinstating of communication pathways	Fulfilled
The areas to be covered include the states of Schleswig-Holstein and Hamburg.	Fulfilled
Able to operate from ground segment within 100NM	Fulfilled
Able to fly second spontaneous emergency scenario	Fulfilled
Operable in several weather conditions and up to 55° latitude	Fulfilled
Probability of a catastrophic fallout is acceptable	Fulfilled
Taking high altitude weather phenomena into account	Fulfilled
Estimation of costs	Fulfilled

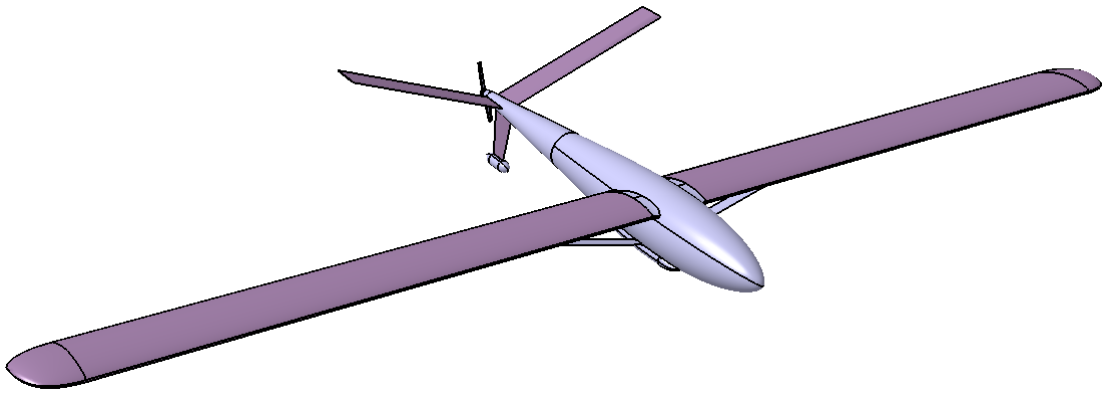

FIGURE 1. Three-sides view of the *Sentinel* aircraft

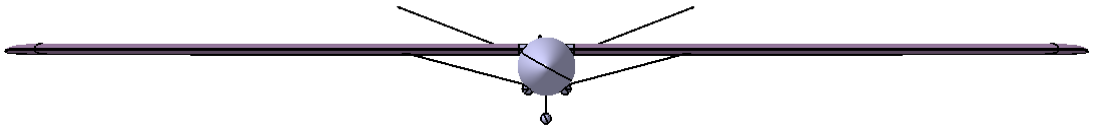

FIGURE 2. Front view of the *Sentinel* aircraft

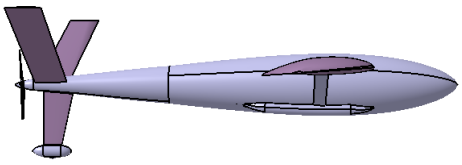

FIGURE 3. Side view of the *Sentinel* aircraft

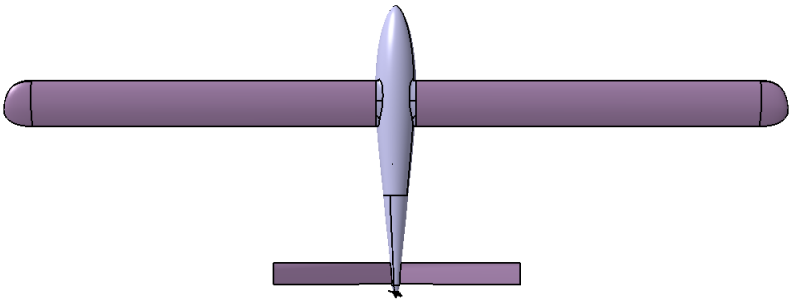

FIGURE 4. Top view of the *Sentinel* aircraft

2. DEFINITION OF THE DESIGN-CONSTRAINING DISASTER

As specified by the requirements, the *Sentinel*-System is meant to operate in a complex environment, under a variety of conditions constrained by an unspecified disaster. However, the nature and extend of the disaster is not further elaborated. Therefore, the following characteristics are defined / derived from the requirements given:

Critical communication infrastructure has been compromised on a large scale, as evident by the requirements of a system to bypass ground-based infrastructure. The following scenarios are considered:

1) A large-scale power outage has occurred and has rendered ground-based communication-infrastructure inoperable.
2) Physical destruction of infrastructure has occurred, mainly cellphone-towers and communication-nodes.
3) Space-based communication infrastructure has been disabled. Either the ground segment has been disabled as described in scenarios 1 & 2, or the space-segment has been rendered inoperable, for example by a solar storm.

The physical destruction of infrastructure, especially in northern Germany is further investigated:

1) A large-scale storm has damaged cellphone-towers, communication-nodes or restricts staff from getting to work
2) Flooding has damaged communication infrastructure or has compromised secondary infrastructure, like transportation or electrical structures
3) Intense rain or snowfall has damaged communication infrastructure or secondary infrastructure

Other desaster cases, such as volcano eruptions generally don't occur in northern Germany and are disregarded. Furthermore, anthropogenic disasters, such as military conflicts are disregarded as well, due to their unpredictability and high safety concerns for the aircraft system as well as personnel.

For the entire system, the following requirements are derived:

1) The system needs to operate continuously with an unstable or disabled electrical grid
2) The system needs to operate in stormy, rainy and cold weather conditions
3) The system needs to operate mostly independent from external infrastructure, in case of physical damage. For example, road access to the operational base might be impossible
4) Certain goods and supplies might be unavailable, for example, certain fuels or spare parts
5) The system needs to operate with a minimum number of personnel to reduce the presence of humans in the disaster area as well as to reduce cost. A part of the personel might be unable to reach the base in case of a desaster

3. DESIGN APPROACH

3.1. Airborne system

The aircraft needs to be designed with respect to the constraints as stated in chapter 2. In general, the aircraft needs to be robust and most importantly, easy to operate and maintain, even under disaster conditions. Wherever sensible, components should be designed in a way so they can be fixed on site or easily replaced from a stockpile. Aircraft parts that need replacement on a regular basis, for example, tires or engine components should be easily obtainable and held in stock.
The same logic is applied to the fuel used (More on self-replenishing systems in chapter 5.3). Certain exotic fuels are not expected to be readily available under wide-spread disaster conditions or cannot be delivered to the operational base (See constraint 3) and 4)).
However, aircraft components that are very hard to repair or replace by nature, for example structural members of the airframe, do not benefit from a stockpile on site, since repairs at a more sophisticated facility would be necessary anyways. These components can therefore be technologically advanced, with degraded capability to be repaired on-site.

General Design Principle (GDP)
Components that break frequently or need to be maintained on a regular basis should be as simple and crude as possible. Components that break rarely and if so, require extensive repairs anyways, regardless of material choice etc., should make use of more recent technologies to increase the overall performance of the aircraft.

4. OPERATIONAL ENVELOPE

4.1. Altitude Envelope

The targeted operational altitude is selected as **18000m** for the following reasons:

1) A local minimum in the average jet-stream velocity exists at around 18000m to 23000m. A lower average wind speed allows the aircraft to be designed with a lower peak velocity. This is of particular interest with regard to the dash into scenario 2 of the requirements, since the potential headwind is weaker.
2) At an altitude of 18000m, the FOV of the relais module can be best utilized. With a half-cone-angle of $45°$, the sensor covers an area of $1017km^2$. If the population density of Schleswig-Holstein is assumed to be uniform, 231282 people are located within this area. At a bandwidth of $0.1\frac{GB}{s}$ per person, each aircraft transmits a data rate of $23.1\frac{GB}{s}$, still leaving room to spare for more bandwith, should the local population density be higher.

4.2. Velocity Envelope

4.2.1. Jet stream considerations

At an altitude of $18000m$ above northern Germany, the aircraft is expected to encounter the polar-front jetstream. This wind phenomenon occurs at all times of the year between latitudes of $40°$ to $60°$ north as well as south. The maximum wind velocity usually occurs between $10km$ and $12km$. The average velocity distribution plotted against altitude of polar-front jet streams is depicted in the following image [1]:

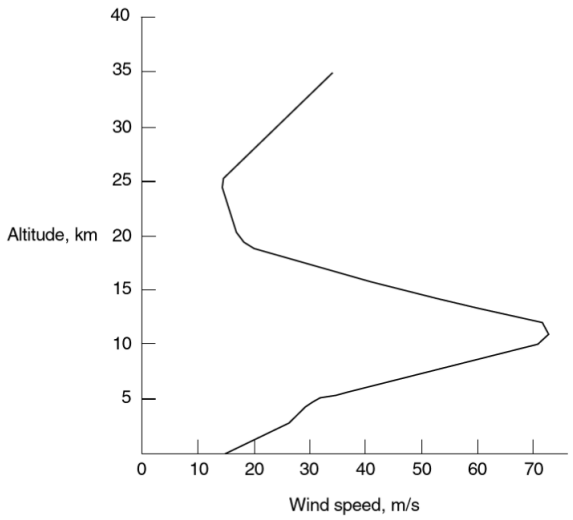

FIGURE 5. Average velocity distribution. Notice the maximum at 12 kilometers

However, 50% of all encountered jet stream velocities are higher than the average. As jet stream data at high altitudes is not readily available over extended periods of time, judging a realistic 'highest design velocity' is difficult. Due to a general lack of data about velocities at $18000m$, the following, conservative approach is used to define a design jet stream velocity:

- The 'Deutscher Wetterdienst' (German meteorological agency) classifies the velocity profile in figure 6 as a **'very strong jet stream'** [1].

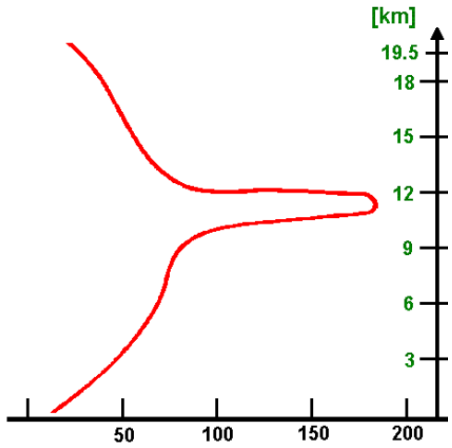

FIGURE 6. A 'very fast jet stream', recorded over central Europe. The velocity scale is in knots [1].

- Furthermore, the German meteorological agency provides the graphic in figure 7 for an 'average jet stream'. Notice how the maximum isn't as constrained to a slim altitude band as the jet stream in figure 6. This 'average' velocity profile is stretched along the velocity scale, until the maximum of the stretched average velocity profile reaches the same velocity as the 'very fast jet stream'.

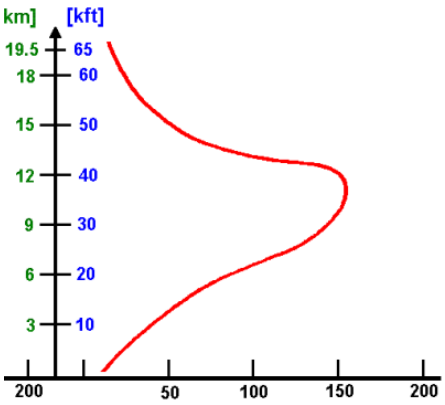

FIGURE 7. An 'average' jet stream velocity distribution. The velocity scale is in knots [1].

- The jet stream velocity at $18000m$ is read from the stretched velocity profile as $23\frac{m}{s}$.
- To make a very conservative estimate, a factor of safety of 2 is applied, leading to a **final design jet stream velocity of** $46\frac{m}{s}$. This is the maximum headwind that will be considered when defining the maximum design airspeed.
- Although in some instances, higher jet stream velocities have been recorded [1], they are regarded as freak occurrences and will not be considered design-constraining.

4.2.2. Top Speed

As the usual wind velocities need to be taken into account at all altitudes, the velocity envelope needs to be defined in consideration of the prevalent wind velocities.
As long as the aircraft is loitering above either scenario 1 or 2, the top air speed needs to be at least as high as the highest realistically expected wind velocity, so distance above ground can be covered in any direction, regardless of wind direction. However, the design-constraining case is the dash into scenario 2:
The distance above ground is given as $170NM$, or $314.8km$ to be covered in two hours maximum. The required above-ground velocity is therefore required to be $43.8\frac{m}{s}$. However, the aircraft might need to fly into a strong headwind, adding an additional velocity component. Using the value of $46\frac{m}{s}$ as obtained in chapter 4.2.1, the maximum airspeed realistically required for the dash into scenario 2 is $46\frac{m}{s} + 43.8\frac{m}{s} = 89.8\frac{m}{s} \approx 90\frac{m}{s}$.

> The aircraft needs to achieve a minimum top air speed of $90\frac{m}{s}$.

4.2.3. Cruise velocity

Once the aircraft is present at $18000m$ above either scenario 1 or 2, the cruise velocity is not constrained by any parameter of the requirements. Although it is desirable that the aircraft is able to loiter semi-stationary above a certain point on the earth, this is not dependant on velocity. Only the loitering pattern needs to be matched to the cruise velocity as well as the location. The minimum cruise speed should exceed the design jet stream velocity of $46\frac{m}{s}$, so the aircraft can cover distance above ground in any direction.

4.2.4. Endurance

The endurance of each aircraft is a result of the number of systems utilized as well as the landing and refueling timing. After a preliminary analysis of the ground segment, a target duration of two days, including ascent to target altitude and descent is selected.

5. AIRCRAFT CONCEPT

5.1. Manned / unmanned debate

Studies resulted in an unmanned approach for the aircraft system. The reasons are:

- A time of flight of two days is incompatible with basic human needs, if the aircraft mass has to be kept in check
  - At least two flight crews are required aboard the aircraft to comply to working hours and flight time restrictions, increasing mass
  - Life-support systems to enable humans to operate an aircraft at $18000m$ add additional mass and complexity, violating the *general design principle*
- The size of the workforce to support the sentinel system increases drastically:
- As 25 aircraft are required to cover the entire area of operations (Chapter 6), a manned solution increases the workforce to support the *Sentinel*-system drastically, as not only pilots, but also additional staff to take care of the human-specific equipment is required
- An unmanned solution includes less critical contingency scenarios
- An unmanned solution allows a higher risk tolerance, as there is not thread to the life of the pilot

5.2. Fuel choice

Two different approaches are investigated for the choice of fuel type:

- Self-Replenishing / high-energy-density concepts, mainly nuclear-fueled and solar-electric propulsion systems
- Propulsion concepts that need regular refueling, with flight duration on the timescale of days or weeks

For the decision-making process, **requirement 1), 3) and 4) as well as the *general design principle*** will be applied.

5.3. Self-Replenishing / high-energy-density concepts

5.3.1. The solar-electric approach

The solar-electric approach envisions an aircraft powered by electric motors, supplied by batteries carried on board, which are recharged by solar panels mounted on the wings during the day.
Although this concept was envisioned as the primary candidate originally, upon detailed simulation a solar-electric aircraft was considered unsuitable to fulfil the requirement of robustness. Due to the short time of sun exposure at the shortest day at $55°$ north, this approach would have resulted in a very fragile aircraft with only $3kg$ of structural mass available per square-meter of wing area. This was deemed to be unsuitable to operate on-demand during most given disaster-conditions.

5.3.2. Nuclear-fueled approaches

Although nuclear-powered aircraft have been proven to be feasible by the Soviets in 1961 [2], it remains to be seen whether the technology will ever reach widespread adoption. For now, this approach will be disregarded due to operational complexity as well as little understood safety hazards. Furthermore, a nuclear-fueled aircraft appears to be a very expensive system to develop and operate.

5.4. Regular-Refueled concepts

5.4.1. Gaseous fuels at room temperature

This category concerns very short-chain hydrocarbons, such as Methane or Propane as well as combinations, like liquefied natural gas (LNG) or liquid petrol gas (LPG) as well as hydrogen. Of those fuels, hydrogen is further investigated, since it offers the highest gravimetric energy density ϕ at $\phi = 120\frac{MJ}{Kg}$ [3].
Common to those fuels are the difficulties in storage. For storage on board an aircraft, a high density is paramount to reduce occupied fuselage volume as well as structural mass by reducing tank size. Two forms of storage are commonly utilized:

- High-pressure storage of the fuel in gaseous form. This approach does not require further active equipment for storage. However, the structural mass of the tanks increases with the storage pressure, greatly reducing the gravimetric energy density of the fuel system, including the fuel itself as well as structural mass.
- Liquefaction of gaseous fuels allows the storage at higher densities, without requiring high-strength fuel tanks. However, this approach has major drawbacks:
  - The fuel tanks need to be actively cooled to reduce boil-off-losses due to heat intake through the tank skin. The cooling equipment adds additional mass to the system. The energy required for cooling must be subtracted from the amount of energy carried in the tank, reducing the effective energy density even further.

– Bulky insulation is required to keep the heat intake through the tanks skin to a minimum. Furthermore, feedlines and fluidic equipment needs to be insulated as well, to avoid excessive vaporization in the entire system.

Considered fuels and their gravimetric energy densities in $\frac{MJ}{Kg}$ [4]:

Fuel type	**Energy density ϕ in $\frac{MJ}{Kg}$**
Hydrogen	120
LNG	53,6
LPG	49,1 / 49,6 (Butane / Propane)

TAB 1. Energy densities

5.4.2. Liquid fuels at room temperature

This category includes all common fuel types, such as kerosene, gasoline or diesel. They are generally characterized as hydrocarbons with medium-length chains. Although they do not offer gravimetric energy densities as high as gaseous fuels, storage requires only light tanks. Some fuels considered are listed with their energy densities ϕ [4]:

Fuel type	**Energy density ϕ in $\frac{MJ}{Kg}$**
Gasoline	46.6
Diesel fuel	45.6
AvGas	44.5
Kerosene	43
Methanol	19.7
Ethanol	30

TAB 2. Energy Densities

Although Methanol and Ethanol offer low energy densities in comparison, they are included since they are prime candidates for use in fuel cells, alongside hydrogen.

5.5. Operational Considerations

Aside from choosing a fuel with the optimal physical characteristics, the special constraints of the scenario need to be taken into account. Although hydrogen infrastructure is expected to be developed further until the entry into service date (EIS), it is unclear how resilient it will be towards the disaster scenarios considered in chapter 2. There are three major violations of the requirements defined in chapter 2 and 3.1:

- Requirement 1) demands operations for extended periods of time independently from the power grid, making storage of liquefied propellant difficult.
- Due to damaged infrastructure, liquefied propellant might either be unavailable for extended periods of time or cannot be delivered to the operational base, violating requirement 3).
- Storage of gaseous propellant under high pressure poses hazards, especially considering the fire and explosion hazards of hydrogen, LNG and LPG and is deemed unsuitable for continued operations under disaster conditions. The gaseous-fueled approach therefore violates the general design approach of simplicity and robustness whenever possible as specified in chapter 3.1. A final decision on the fuel type will be taken together with the engine type.

Requirement	1	3	4	G.d.Principle	$\phi_{fuel}/\phi_{system}$
Hydrogen	–	-	0	–	++ / -
LNG	-	-	0	-	+ / -
LPG	-	-	0	-	+ / -
Gasoline	+	+	+	0	+ / +
Diesel fuel	+	+	+	0	+ / +
AvGas	+	0	+	+	+ / +
Methanol	+	0	+	+	- / -
Ethanol	+	0	+	0	0 / 0

TAB 3. Fuel Decision Matrix, see requirements (2)

Some notes on the scores given in the decision matrix:

- As there are no further permits for combustion-engine cars to be given after 2035 [5], gasoline and diesel availability will decrease thereafter. However, the available supply can be sourced at any gas station.
  On the other hand, AvGas and *sustainable aviation fuel* (SAF) equivalents are expected to stay in use for some time longer, but is generally only available at airfields.
  Therefore, all three fuels are rated '+' for requirement 4, but gasoline and diesel are considered to be more easily accessible for requirement 3.
- The same is assumed to apply to Methanol and Ethanol, although it is not as clear where the future of those fuels is headed.

> Although liquefied gaseous propellants offer higher base energy densities than the more conventional liquid fuels, they are deemed unsuitable under operational conditions as well as for storage system structural mass. They will not be investigated further.

5.6. Propulsion system

5.6.1. Methanol / Ethanol Fuel cells

As hydrogen as a fuel has been ruled out in chapter 5.5, Methanol and Ethanol remain to be investigated for use in fuel cells. As for the rest of the propulsion system, the electric motor is assumed to have an efficiency of $\eta = 0.95$ [6], for the propeller, $\eta = 0.85$ is used [7].
For using Methanol in a Direct-Methanol Fuel Cell (DMFC), efficiencies of $\eta = 0.2 - 0.3$ are achieved, leading to a propulsion system efficiency of $\eta = 0.24$. It is to be noted that cell efficiencies of up to $\eta = 0.44$

appear possible under perfect conditions, albeit with low power densities [8].

Efficiency-wise, Direct-Ethanol Fuel Cells are on par with DMFC's, however, the base energy density of Ethanol is about 1,5 times higher than Methanol, making them superior for airborne applications.

Considering the overall propulsion system efficiency, which is not expected to succeed $\eta = 0.35$ until the EIS date, fuel cells do not appear to be a viable form of propulsion, especially considering the additional weight and complexity of the aircraft, which is to be avoided by the *general design principle*.
From an ecological point of view, fuel cells do not avoid emissions of CO_2-Gas. Therefore, there is little difference between reacting Methanol / Ethanol in a fuel cell or combusting it directly in a piston - or turbine engine.

> DMFC's and DEFC's do not offer significant advantages from an energetic and ecological point of view over directly combusting the fuels. Additionally, the fuel cells add additional weight to the aircraft. They are therefore not considered viable forms of propulsion.

5.7. Combustion devices

Aside from electric motors, piston engines, turboprops as well as turbfans are investigated. Turbojet engines only offer benefits at high speeds, which are not to be encountered during the planned mission.

Requirement	2	3	4
Piston	0	+	+
Turboprop	0	-	0
Turbofan	0	-	-
Turbojet	0	-	-

TAB 4. Propulsion system decision matrix, see requirements (2)

5.8. Engine selection

As piston engines offer the best option for the given requirements, the issue of low performance at altitude need to be addressed. Coincidentally, the NASA research aircraft *Perseus B* uses at triple-charged *Rotax 914* engine. It produces $105hp$ $(78.3kW)$ at $60000ft$ $(18300m)$ [9].

Either a future development of this engine or a new engine design with similar performance characteristics, which might be developed until the EIS date, is to be used for the *Sentinel* aircraft. Either one or multiple engines are to be used, depending on the aircraft configuration. By choosing the *Rotax*-engine, the fuel *AvGas* or an SAF equivalent will be used.
Common gasoline-engines for small general aviation applications, such as the *Rotax 912* and the *Rotax 914* achieve total engine efficiencies as high as $\eta = 0.3$ at ideal power settings [10].

6. OPERATIONAL CONCEPT

6.1. Operational Base

The operational base concept as well as the flight plan is paramount for smooth operations in both scenarios. Its tasks include the stationing of personnel as well as the accommodation, maintenance, and refueling of the aircraft. Additionally, during flight phases, all aircraft are monitored and controlled by controllers from the base.

To meet these requirements, multiple hangars are needed to safely store and handle the 25 aircraft in continuous operation for scenario 1, along with providing two reserve aircraft. Similarly, to handle of aircraft, each piece of equipment is placed on a hall trolley, which can be moved within the operational base using a forklift. A basic concept of such a trolley can be seen in Figure 8.

FIGURE 8. Trolley [11]

Furthermore, a fuel depot ensures that autonomous operation is possible in the event of a disaster. Based on the cumulative fuel consumption of the aircraft and the base, an estimated 11800 kilograms of gasoline are required. This amount is needed to simultaneously refuel 27 aircraft with 400 kilograms of gasoline each. Similarly, the operational base has a reserve of 1000 kilograms of gasoline to ensure a power supply through generators in the event of a power outage. The electrical supply is to be supplemented by solar / wind energy at the base. However, emergency generators are to be sized to fully supply the base in case there is no green electricity available. To obtain and maintain such a quantity of fuel, the operational base is also equipped with its own fuel tanker, which replenishes the base's fuel reserves from official supplies, or gas stations during supply emergency. For communication between aircraft and controllers, the operational base is equipped with air traffic control equipment. Decisions regarding the deployment plan for individual aircraft, their maintenance, or mission objectives are taken on base.

Aircraft mechanics are employed for the maintenance of the planes, who are guided by an engineer. The number of employees required for operations depends on scenario 1, as covering a large area requires more effort than a time-critical deployment of a single aircraft.

For this scenario, the following employees are required:

1 x Truck Driver
5 x Systems Engineer
1 x Logistics Specialist
2 x Aircraft Mechanic
1 x Aerospace Engineer

The tasks of the employees are distributed as follows:
Truck driver: Supplying the base with sufficient fuel;, transportation of aircrafts and components
Systems engineer: Controlling the aircraft in flight and after clearance for takeoff, monitoring all relevant systems of individual aircraft
Logistician: Coordination of aircraft handling (loading and unloading), potentially coordinating the procurement/installation of spare parts
Flight equipment mechanic: Conducting all necessary visual inspections before clearance for takeoff, performing planned and unplanned maintenance and repairs of aircraft

To be able to quickly reach and cover the Schleswig-Holstein and Hamburg deployment area, the Rendsburg-Schachtholm airfield (ICAO identifier: EDRX) is chosen as the location for the operational base. This location is ideal for the missions because it is close to larger cities like Kiel, ensuring a reliable fuel and parts supply.
Furthermore, the airfield has the necessary infrastructure of fuel depots and hangars. Additionally, the airfield features a 960-meter asphalt and a 600-meter grass runway. [12]
Aircraft can take off from these runways in a staggered manner. The airfield is suitable for the takeoff and landing of aircraft with a maximum takeoff weight of over 3 tons, which means that *Sentinel* is able to take off from there. [12] Moreover, the runway orientations 03/21 and 12/30 ensure that aircraft can take off without significant crosswind components.

6.2. Operational Procedure Scenario 1

The area to be covered in Scenario 1 encompasses Hamburg and Schleswig-Holstein, with a total area of over 16000 km^2, aiming to provide internet access to over 4 million people. Given that the aircraft flies at an altitude of 18 km above ground level during the loiter phase, assuming that the areas are at sea level, 25 aircraft are required to ensure coverage. The deployment areas for each aircraft are depicted in Figure 9.
Each aircraft covers a circular area with a radius of 18 kilometers. The circular area is $1017km^2$. This poses a challenge in the greater Hamburg area, as multiple relay modules need to be installed on each aircraft to ensure

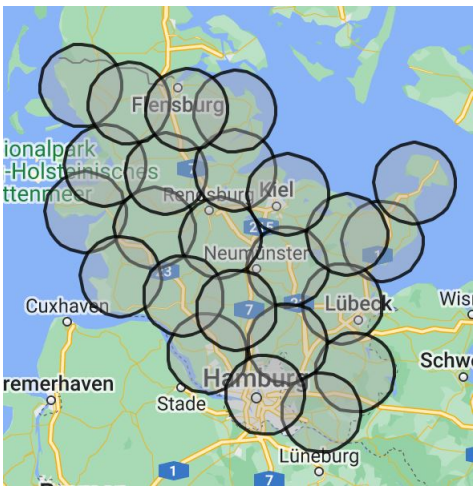

FIGURE 9. Internet relais coverage

that the number of people within a coverage area receives a minimum data speed of 0.1 Mbps. Consequently, the aircraft has been designed to accommodate eight relay modules per aircraft, with seven being required for Hamburg.

The deployment process for the given Scenario 1 is composed of several individual phases that follow a standardized procedure before each operation.

Special attention has been given to minimizing the time required to restore internet connectivity when designing the deployment plan. As a result, the decision was made to locate the operational base in close proximity to Hamburg, just before reaching the disaster area.
As shown in figure 10, it is assumed that approximately 6 hours will elapse from the time the mission is assigned until the aircraft take off from the airfield. The timing of the phases is shown in figure 10.
The phases are described in the following:

- First phase: Mission order is received at the operational base and is communicated to the personnel
- Second phase: Majority of personnel driving aircrafts out of hangar by using a forklift;
- Third phase: opening fuel bunker; refueling aircrafts
- Fourth phase: disassembled aircraft could be reassembled by using a quick connector mechanism
- Fifth phase: All parts of the aircraft undergo a visual inspection to ensure their airworthiness while being refueld
- Sixth phase: Manually executed phases are completed; System engineers take control over the aircrafts
- Seventh phase: System engineers start rolling procedure and line up aircrafts at runway
- Eight phase: Aircrafts start from runway

One possibility that this schematic deployment procedure allows for is that the aircraft with the longest distance to the respective deployment area will take off first. This ensures that the aircraft will take off in staggered intervals based on their travel distance, ensuring that the entire deployment area is provided with internet access simultaneously.

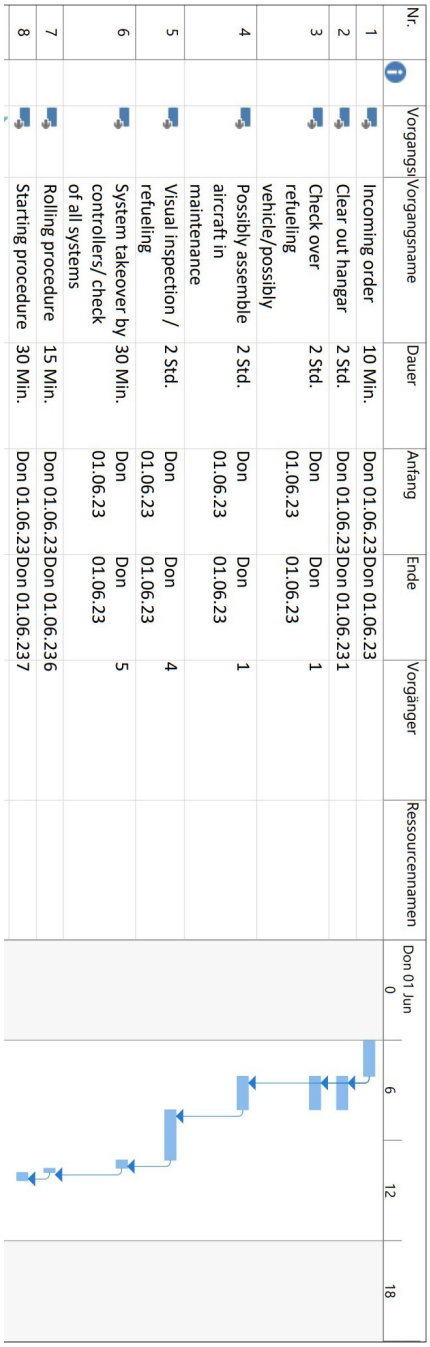

FIGURE 10. Operational plan

6.3. Operational Procedure Scenario 2

Scenario 2 presents a local time-critical mission of a single aircraft. The communication link over a circular area of $700km^2$ is to be reestablished within two hours. Following the arrival, the aircraft enters a loitering pattern. Aircraft control is equivalent to scenario 1. Any aircraft can be used for the second scenario since all aircraft carry both a radar as well as internet relais. One aircraft covers an area of 1017 km^2 with the radar module and is sufficient to supply scenario 2.
As one aircraft is removed from scenario 1, it needs to be replaced by launching a new one. The time to remove the aircraft from the hangar is reduced to approximately 10 minutes. Similarly, the time required for refueling and visual inspection is expected to be around 15 minutes. As only one aircraft is required, the assembly of an aircraft is not necessary. Furthermore, the aircraft's takeoff time after the taxi phase is estimated to be one to two minutes. Therefore, it can be stated that under the same conditions as in Scenario 1, the aircraft will be airborne after approximately one hour.

6.4. Maintenance in continuous operation

Maintenance during continuous operation presents the greatest logistical challenge. It has to be ensured that aircraft undergoing maintenance can only land when there are ready-to-use aircraft available to take their place.
In the context of this project, the maintenance primarily focuses on the *Rotax 914* engine. According to the manufacturer's guidelines, the engine should undergo an initial inspection after 25 operating hours, followed by subsequent inspections every 100 operating hours with a deviation of +-10 percent. [10] The abstract of the maintenance guide is shown in Figure 11. These

	Intervall - Stunden									
	25 h	100 h	200 h	300 h	400 h	500 h	600 h	700 h	bis	2000 h
100 h	X	X	X	X	X	X	X	X		X
200 h			X		X		X			
600 h							X			

FIGURE 11. Abstract of Rotax maintenance guide [10]

inspections are considered routine maintenance. During these inspections, the manufacturer specifies that the following areas should be thoroughly examined:

- General visual inspection of the engine for damage
- Visual inspection of temperature and oil pressure sensors
- Inspection of cooling hoses
- Checking the expansion and overflow tanks for damage
- Inspection of oil lines for damage
- Inspection of fuel lines for damage
- Inspection of wiring and connections
- Inspection of the exhaust system for cracks

These inspection procedures ensure that the engine is in proper working condition and any potential issues are identified and addressed promptly. The maintenance team at the operational base follows the manufacturers guidelines meticulously to maintain the reliability and performance of the engines throughout the continuous operation. [10]
For the 100-hour inspection, it is assumed that an aircraft mechanic requires a time of two hours to perform maintenance on one aircraft engine. Therefore, with the two available spare aircraft, two aircraft can always depart from the operational area and be replaced by the spare aircraft. By taking advantage of the manufacturer's 10 percent rule and utilizing the two spare aircraft, every two hours, two aircraft can depart from the operational area and be exchanged with the ones that have undergone maintenance. This process continues until all 100-hour inspections are completed. Additionally, the maintenance system has flexibility in its applicability in case of maintenance delays, as ideally, all aircraft would

be maintained after approximately 13 hours. According to the manufacturer's specifications, a maintenance window of 20 hours is available during continuous operation.

In general, it should be noted that the manufacturer specifies a time interval for major overhauls, which, for this type of engine, is based on either a total flight time of 1000 hours or a period of 10 years, whichever comes first.

In addition to the routine engine inspections, it is determined that a visual inspection for damage must be conducted on the entire aircraft before and after each flight. If any damage is detected, it is repaired, and the spare aircraft come into use. To minimize maintenance times in case of damage, individual components can be replaced directly with available spare parts at the operational base, thus repairing only the damaged components. The aircraft is designed such that the fuselage and wings are separate components that are assembled during aircraft upgrades. Therefore, in the event of, for example, wing damage, it is possible to replace the wing and repair the damaged wing separately while the aircraft remains operational by exchanging it with a spare wing.

Nevertheless, the maintenance of the airframe also includes routine inspections, including the annual aircraft inspection and the 3000-hour inspection. The annual inspection demonstrates the airworthiness and full functionality of the aircraft. As an additional safety measure to assess the effects of sustained loads on the airframe, an additional test is conducted every 3000 hours, during which the entire aircraft, including all individual components, is inspected for damage. During these inspections, it is not possible to accept orders for restoring internet connectivity.

6.5. Estimation of Costs and Provision of Continuous Operation

The costs for providing continuous operation can be categorized into the following sectors:

-Fixed costs of the operational base
-Employee costs
-Fixed costs of technical equipment
-Costs for manufacturing the aircraft and their spare parts
-Maintenance costs for the aircraft and the operational base during operation
As fixed costs for the Rendsburg-Schachtholm airfield base, an estimated location rent of 50000 euros per month is assumed. Employee salaries are based on the variable hourly rates specified in the collective bargaining agreements of *IG Metall*, with the variable hourly rates for each employee as follows:

Aerospace Engineer: €120/hour
Systems Engineer: €120/hour
Aircraft Mechanic: €70/hour
Logistics Specialist: €70/hour
Truck Driver: €50/hour

Based on a 40-hour workweek, the annual employee costs amount to €2038400. Besides employee costs, the main cost factor is the manufacturing of the aircraft and their spare components. The General Atomics MQ-1 Predator drone has a unit price of approximately 4 million US-Dollars. [13] Considering that the functionalities of the *Sentinel* are significantly more limited compared to a military drone, the Stemme S-12G is used as another comparison aircraft, with a unit price of approximately €400000. [14]Thus, it can be noted that a significant portion of the manufacturing costs is attributed to the complex controls and electronic devices in the drone. Based on this, the production cost of a *Sentinel* drone is estimated at €1.5 million. It is assumed that the procurement of spare parts includes a wing costing €300000 and a fuselage costing €900000. It is further assumed that in the event of damage, all technical components of the spare parts, such as the Rotax engine in the fuselage or the propeller, need to be replaced. Therefore, for continuous operation, 27 aircraft are manufactured (25 for radar coverage in Scenario 1 + 2 aircraft as replacements during maintenance), and two additional aircraft are provided as spare parts for the operational base. Thus, the manufacturing cost of all aircraft and spare parts amounts to €43.5 million. In addition to the manufacturing costs, the acquisition of a truck and a tanker, each valued at €150000, and a forklift valued at €100,000 are included.

The ongoing costs mainly consist of fuel costs due to the consumption of the operational base and the aircraft, as well as liability insurance for each aircraft. For a flight mission following Scenario 1, the fuel consumption is estimated at 11,800 kg of gasoline. Considering a density of 0.74 kg/L for gasoline, this corresponds to approximately 15946 liters. Assuming a gasoline price of €1.80 per liter, the fuel costs would amount to €28703.

In summary, the cumulative fixed costs amount to €43.9 million. The annual employee costs total €2038400, the rental costs amount to €600000 per year, and the consumption costs of the base per mission are €28703.

6.6. Possibilities for use outside the scenarios

The aircraft have additional areas of application beyond the described scenarios. Due to their operating altitude of 18 kilometers, they are well suited for surveillance and detection of large areas, making them ideal for monitoring and detecting natural disasters.
An alternative use would be wildfire detection over an area the size of Schleswig Holstein and Hamburg. By replacing the internet relays with infrared sensors for heat detection, the 'Sentinel' could be used to trigger an alarm in case of elevated ground temperatures, enabling early fire detection. Synergies with the systems of the 2022 DLR-Challenge are possible,
As already described in the scenarios, continuous operation of the aircraft fleet is possible, enabling

communication to affected individuals. The same applies to other natural disasters such as floods or earthquakes. Due to the interchangeability of the internet relays with other electronic components, the aircraft can be used to establish an early warning system for various natural disasters.

In addition to civilian applications, military applications are possible. Due to their high operating altitude, the aircraft are also suitable for gathering reconnaissance information over an operational area or transmitting signals. However, due to the limited payload of the aircraft, which is required to ensure a continuous flight duration of two days, they are less suitable for carrying or dropping objects during flight. Nevertheless, this could be feasible on a smaller scale.

7. GUIDANCE & NAVIGATION

As the aircraft is planned to operate unmanned, particular attention is paid to guidance and navigation to ensure safe and reliable operation.

7.1. Guidance

The aircraft adjusts it's position and orientation in all dimensions semi-autonomously. As the flight profile itself is not particularly complicated, an air traffic controller at the operational base does not directly interfere with the flight controls. Instead, the controller is expected to *tell* the aircraft where to fly or defines waypoints which the aircraft follows automatically.

> An aircraft / air traffic controller at the operational base is expected to *deploy* the aircraft's capabilities instead of *flying* the aircraft

However, this semi-autonomous approach requires a capable flight control system on board of the aircraft, consisting of sensors, computers and controllers, to make adequate control surface inputs. The guidance & navigation logic is briefly explained in the following chapters.

7.1.1. Aerodynamic guidance

Orientation relative to the airstream is determined by the typical aircraft sensor package, consisting of pitot tubes, angle of attack sensors and pressure transducers. The data acquired from these sensors is used to fly the aircraft in a stable and controlled manner.

7.1.2. Spatial orientation

To determine the orientation of the aircraft relative to the earth-surface reference frame (ESRF), more or less constant vector fields as references are required. In order to accomplish this, an attitude determination platform will be used.
Attitude can be determined by the three Euler angles between the earth-surface reference frame and the aircraft reference frame (ARF). The orientation of these reference frames relative to each other can be described by the transformation matrix $\bar{T}_{21}(\phi, \theta, \psi)$. The Euler angles ϕ, θ and ψ are the orientation angles of the aircraft:

Angle	Aircraft orientation
ϕ	Roll angle
θ	Pitch angle
ψ	Yaw-Angle

TAB 5. Euler-angles between the ESRF and ARF reference frames

By measuring two field vectors in both the ESRF and ARF reference frames, the transformation matrix can be calculated, for example, by making use of the *TRIAD*-algorithm [15]. As has been demonstrated by *Stoll, Kirchner, Braun and Kisch*, a viable attitude determination platform making use of the *TRIAD*-algorithm can be constructed to measure the Euler angles between sensor platform and the surface of the earth. In this case, the magnetic and gravitational field vectors have been measured. A similar system, although more mature until the EIS date, is to be installed on board the aircraft to determine spatial orientation.
The following reference vectors are to be used:

- The gravitational vector in the ARF $\vec{a}_{ARF}$ is to be measured by an accelerometer on board the aircraft
- The gravitational vector in the ESRF can be assumed to be $\vec{a}_{ESRF} = [0; 0; 1]^T$

- The second vector to be measured is the magnetic field of the earth. It is to be measured by a three-axis magnetometer on board the aircraft in the ARF, $\vec{B}_{ARF}$
- The magnetic field vector in the ESRF, $\vec{B}_{ESRF}$ is either assumed to be a constant magnetic field for the entire operational area, resulting in less accurate orientation results. Alternatively, the earth's magnetic field can be uploaded as a map onto the aircraft's computer

By measuring and comparing these four vectors at any time, the attitude of the aircraft relative to the surface of the earth can be determined.

7.2. Navigation

While guidance concerns the attitude of the aircraft and ways to control and change the spatial orientation, the aim of navigation is to determine the position of the aircraft, and to a further extend, the state vector $\vec{S}$:

$$(1) \qquad \vec{S} = \begin{bmatrix} \vec{K} & \dot{\vec{K}} \end{bmatrix}^T = \begin{bmatrix} x & y & z & \dot{x} & \dot{y} & \dot{z} \end{bmatrix}^T$$

In the following chapters, the means through which the 6 components of the state vector are determined will be described.

7.2.1. Primary navigation

The primary navigation mode relies on a constant radar vector $\vec{R}$ to the aircraft to be uploaded via a data link. A radar at the operational base is to be used to measure the

distance as well as the direction of the aircraft relative to the radar. As the geographic position of the radar $\vec{P}$ is known, the position $\vec{K}$ of the aircraft can be determined, fixing the first three components x, y and z of the state vector:

$$\vec{S} = \begin{bmatrix} P_x + R_x & P_y + R_y & P_z + R_z & \dot{x} & \dot{y} & \dot{z} \end{bmatrix}^T \tag{2}$$

As the altitude of the aircraft might not be determined to the required accuracy via the base radar, the on-board radar of the payload is to be used to supplement the primary navigation solution by measuring altitude above ground on board the aircraft.
To determine the differential of the position vector, multiple radar measurements are to be combined to solve the following differential for each loop of the guidance algorithm:

$$\dot{\vec{K}} = \begin{bmatrix} \dot{x} & \dot{y} & \dot{z} \end{bmatrix}^T = \frac{d}{dt} \begin{bmatrix} x & y & z \end{bmatrix}^T \tag{3}$$

If the time between two radar measurements is Δt, the backwards-facing differential can be approximated:

$$\dot{\vec{K}}(t_0) \approx \left(\vec{K}(t_0) - \vec{K}(t_0 - \Delta t) \right) \cdot \frac{1}{\Delta t} \tag{4}$$

The shorter the revisiting time Δt, the more accurate the change in velocity can be calculated.

> The methods mentioned above describe the usual procedure to determine the aircraft's state vector. This method is to be used as long as there is a radar - and data link connection between the aircraft and the operational base.

7.2.2. Required Antenna / Radar height

As an aircraft is expected to venture far out from the operational base, the radar horizon needs to be considered as a constraint that allows a direct line-of-sight (LoS) connection to the aircraft. As specified by the requirements, the following maximum distance between the operational base and the aircraft is assumed:
$100NM$ need to be covered from the operational base to reach scenario 1. Another $170NM$ is required for scenario 2, leading to a maximum distance of $270NM$ or $500Km$. At an aircraft altitude of $18000m$, a direct LoS is required.
To determine whether a direct LoS is given, the intersect points between the LoS as well as the surface of the earth is calculated.

The surface of the earth can be modeled in a 2D-case by the following equation:

$$E = \sqrt{R^2 - x^2} \tag{5}$$

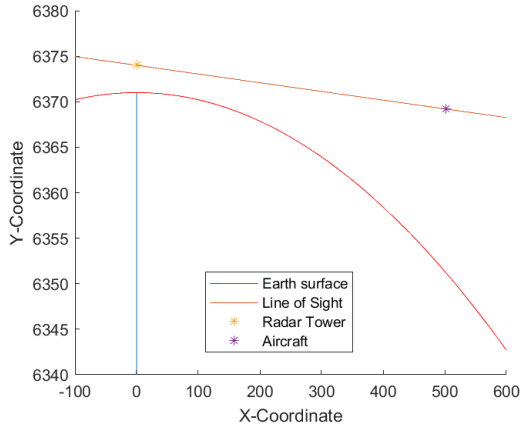

FIGURE 12. LoS geometry, axis ratio not to scale

The LoS is modeled as a linear equation, with R being the radius of the earth, h being the height of the radar at the ground station and d being the great-circle distance between the ground station and the ground point of the aircraft ($500Km$):

$$LoS = R + h + x \cdot \frac{R \cdot cos\left(\frac{d}{R}\right) - (R + h)}{R \cdot sin\left(\frac{d}{R}\right)} \tag{6}$$

If the equation $E = LoS$ is solved for x and plotted against h (The analytic solution is too long to be shown here), there exist two points in which both solution functions assume the same value. In those two cases, the LoS is tangent to $E(x)$. The solution at the smallest x-value describes the case in which the LoS is tangent to $E(x)$ between the position of the aircraft and the ground station. This point represents the valid solution.

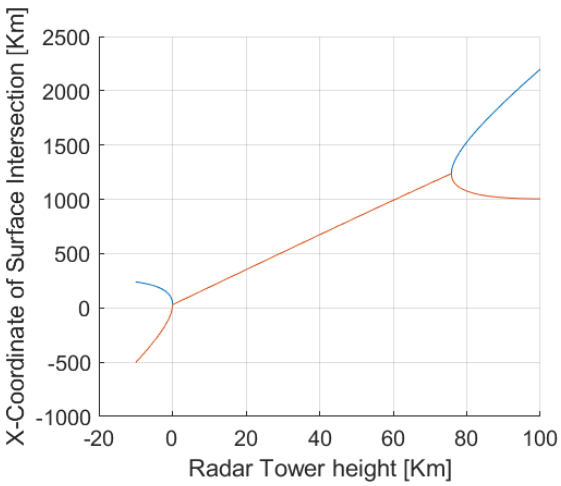

FIGURE 13. Solution of $E = LoS$

Therefore, the minimum height at which the radar needs to be placed is $0,053Km = 53m$. However, due to terrain obstruction, the radar tower should be placed a bit higher.

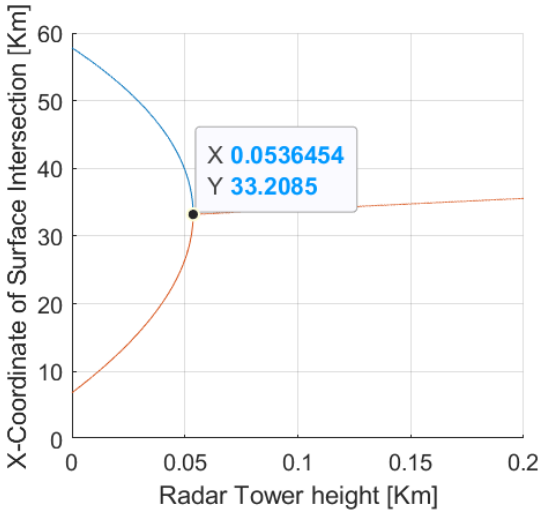

FIGURE 14. Closeup of the relevant solution

7.3. Degraded guidance / contingency scenarios

To account for the inherit risk of technical systems to malfunction as well as the demanding operational considerations, a backup guidance solution is incorporated into the design.
The degraded guidance solution assumes that either the radar or data link to the operational base is broken. This might be the case through:

- A technical malfunction at the operational base
- A technical malfunction on board the aircraft
- The aircraft dives below the radar horizon, for example, during an emergency descent

To minimize risk to humans and infrastructure on the ground as well as the aircraft, the following guidance solution is implemented:

7.3.1. INS navigation

An inertial navigation system (INS) is a device which measures linear acceleration in all three spatial dimensions as well as angular velocity around all three axis. By integrating the obtained values against time, the position and orientation of the INS may be dead-reckoned from a known starting point. INS's find extensive use and spacecraft, aircraft and guided missiles to obtain a position, without external references. Issues associated with INS navigation is the inherit drift of the platform, due to limitations of measurement accuracy's as well as the error in numeric integration methods.
The aircraft is to be equipped with redundant INS's to act as a backup navigation system in case of a loss of radar - or data link contact with the operational base. For this purpose, the state vector obtained by primary navigation is continuously updated to the INS. Should primary navigation fail, the INS takes over with an up to date state vector.
The INS measures the acceleration vector $\vec{a}$ with a time interval of Δt:

$$\vec{a} = \begin{bmatrix} a_x & a_y & a_z \end{bmatrix} = \begin{bmatrix} \ddot{x} & \ddot{y} & \ddot{z} \end{bmatrix} = \ddot{\vec{K}} \tag{7}$$

To obtain a new entry for the derivative part of the state vector, a numeric integral is calculated for every axis:

$$\dot{\vec{K}}(t_0 + \Delta t) \approx \dot{\vec{K}}(t_0) + \ddot{\vec{K}}(t_0) \cdot \Delta t \tag{8}$$

To calculate a new position, another integration step using the velocity vector at $t = t_0$ is performed:

$$\vec{K}(t_0 + \Delta t) \approx \vec{K}(t_0) + \dot{\vec{K}}(t_0) \cdot \Delta t \tag{9}$$

Therefore, the result of one full INS cycle is as follows:

$$\vec{S} \approx \begin{bmatrix} \vec{K}(t_0) + \dot{\vec{K}}(t_0) \cdot \Delta t & \dot{\vec{K}}(t_0) + \ddot{\vec{K}}(t_0) \cdot \Delta t \end{bmatrix}^T$$

7.4. Close-Range navigation

In order to make emergency landings after an engine failure or during any emergency situation, the LoS link with the operational base will be lost, as the aircraft descents below the radar horizon. Although the aircraft is able to navigate to a large field, suitable for a landing using INS navigation, it must be determined whether there are temporary obstacles present that do not allow a landing, for example, agricultural equipment.
To deal with this issue, a small camera is to be included. The video feed is to be analysed by the on-board computers to determine whether a safe landing is posible.
The same method will be used to navigate towards the operational base, if primary navigation has failed. Although the aircraft is able to accurately navigate into the vicinity of the operational base, the close-in approach is flown with support from image analysis of the camera.

7.5. Redundancy & Component choice

All guidance hardware on board the aircraft is redundant in a voting configuration. This means that three guidance computers as well as three INS platforms are carried. If one system output is different to the two other systems, it is voted out. In case of physical failure, e.g. a system component going offline, two backups are still available. It is decided that this approach to redundancy offers the best compromise between safety and weight.
As an INS platform, the *LASEREF VI* by Honeywell is chosen for it's low weight of $4,5Kg$ and a low power draw of $20W$ [16].
For the same reasons, the *VECTOR-MCC* flight computer by *UAV Navigation* is chosen, with a mass of $0.16Kg$ and a power draw of $2.5W$ [17].

8. FLIGHT PROFILE SIMULATION

To simulate different aircraft configurations to determine their ability to fulfil the flight envelope requirements as specified in chapter 4, the following input parameters are required:

- Single-value parameters
  - Aerodynamic coefficients

  - Wing area A
  - structural mass (excluding payload) m_{struct}
  - Fuel mass at takeoff m_{fuel}
  - Payload mass m_{pld}
  - Payload power P_{pld}
  - Specific energy density of the propellant ϕ
  - Total efficiency of propulsion system η
  - Airfield elevation, operational altitude
- Vector parameters
  - Altitude profile $\vec{v}(t)$
  - Velocity Profile $\vec{h}(t)$

To characterize a certain aircraft configuration, the following output values are of interest:

- Single-Value output parameters
  - Time of flight
  - Maximum angle of attack encountered during the simulated flight profile
  - Maximum engine power required during the simulated flight profile
- Time-dependant output parameters
  - Energy on board
  - Airborne mass
  - Angle of attack
  - Aerodynamic drag
  - Power required for altitude changes
  - Total engine power
  - Fuselage equilibrium temperature

The simulation approach relies upon the approximation that every flight state is horizontal, meaning that lift equals weight. Obviously, this is not the case during ascend and descent. Therefore, the energy requirement for changes in altitude is regarded separately. Power due to acceleration, deceleration as well as turns is not simulated, as it isn't expected to be a significant factor in the mission profile.

The flight envelope will be simulated numerically, with the equations being solved for each time $t+dt$, using the values from the previous step at time t. The algorithm at time t_0 goes as follows:

1) The local density is calculated from the altitude function, using the standard atmosphere is calculated:

$$\rho(t_0) = f(h(t_0))$$

2) The airborne mass is calculated:

$$m_{tot}(t_0) = m_{struct} + m_{pld} + m_{fuel}(t_0)$$

$m_{tot}(t)$ is plotted against time as the airborne mass. Using the values $m_{tot}(t_0)$, $v(t_0)$, $\rho(t)$, A and c_{A_α} as well as the angle of attack for zero coefficient of lift, α_0, the angle of attack $\alpha(t_0 + dt$ at $t_0 + dt$ is calculated:

$$\alpha(t_0) = 2 \cdot \frac{m_{tot}(t_0) \cdot g}{\rho(t_0) \cdot v(t_0)^2 \cdot A \cdot c_{A_\alpha}} - \alpha_0$$

α is plotted against time.

3) Using $\alpha(t_0)$, the drag coefficient at t_0 is calculated:

$$c_w(t_0) = c_{w_\alpha} \cdot \alpha(t_0) + c_{w_0}$$

The drag at t_0 is calculated:

$$W = \frac{1}{2} \cdot v(t_0) \cdot A \cdot \rho(t_0) \cdot c_w(t_0)$$

W is plotted against time.

4) From the drag force as well as the velocity at t_0, the aerodynamic power P_a is calculated:

$$E = W \cdot v$$

$$P_a = \frac{d}{dt} s \cdot W(t_0) = v(t_0) \cdot W(t_0)$$

The aerodynamic component of P_a is only one component of the total power required at a certain time t_0. Altitude changes require additional potential power P_p as well.

5)

$$P_p = m_{tot} \cdot g \cdot \frac{dh}{dt} = m_{tot} \cdot g \cdot (h(t_0 + dt) - h(t_0)) \cdot \frac{1}{dt}$$

P_p is plotted as the potential power as a function of t.

6) Additional power is not calculated from the flight profile and includes the power requirement of the payload P_{pld} as well as power P_{misc} for additional on-board systems. Total required power equates to:

$$P_{tot} = P_a + P_p + p_{pld} + P_{misc}$$

All required power on board is supplied by the engine via propulsion or via an alternator. As propellers and alternators generally achieve $80\% - 90\%$ efficiency, the same η is assumed for both power trains. Engine power therefore equates to:

$$P_{eng} = \frac{P_{tot}}{\eta}$$

P_{eng} is plotted against time and shows the total power the motor needs to supply.

7) As the energy used per timestep can be calculated as by $\Delta E = P_{eng} \cdot dt$, the fuel usage Δm for each dt can be calculated using the gravimetric energy density of the propellant, ϕ:

$$\Delta m = \frac{\Delta E}{\phi}$$

A new, resulting m_{tot} is calculated:

$$m_{tot}(t_0 + dt) = m_t ot(t_0) - \frac{\Delta E}{\phi}$$

This new value of m_{tot} is used for the next iteration of the simulation algorithm. The aircraft runs out of fuel when $m_{tot} = m_{struct} + m_{pld}$.

By defining certain flight profiles by defining the vectors $v(t)$ as well as $h(t)$, ascent, descent as well as dash into scenario 2 can be simulated. Furthermore, the loss of fuel mass on board the aircraft can be compensated by varying the velocity during cruise.

Aircraft configurations are considered valid, if the time of complete fuel exhaustion occurs after the aircraft has landed, as by the altitude - and velocity profile.

The flight profile simulation has been tested using ap-

proximations of real aircraft with similar flight envelopes, such as the *U-2*. The time of flight was usually simulated within 15% to 20% of the stated endurance of each aircraft.

8.1. Desirable design traits

Some general technical constraints are limiting possible aircraft configuration:

- The stall angle α_{stall} can never be exceeded. Depending on the flight state, a smaller or greater margin of safety should be achieved.
- Total fuel mass required for the mission should be minimized to:
  - Minimize environmental impact
  - Reduce costs
- Ascent and descent to the operational altitude should be as quick as possible, to increase the time of maximal aerial coverage.
- Takeoff and landing velocities should be low, to increase safety as well as reduce wear on the aircraft.
- The payload consists of 7 broadband relais modules, one radar as well as the two specified antennas. Total payload mass is $43Kg$, with a peak power of $3950W$. As it is not specified for how long the aircraft needs to remain over scenario 2, it is assumed that the entire payload package is run continuously.
- From a systems-engineering-perspective, a total time of flight of two days should be achieved with a full payload

8.2. Assumed values for aircraft components

- The gravimetric energy density of AvGas / Gasoline is assumed at $44,5\frac{MJ}{KG}$ [4]
- The propeller efficiency is assumed as $\eta = 0,85$. Although efficiencies as high as 95% are possible for ideal revolution speeds, the average efficiency during the flight profile is lower [18]
- The efficiency of aircraft piston engines is expected to reach $\eta = 0.35$ by the EIS date. In combination a propulsion system efficiency of $\eta = 0.85 \cdot 0.35 = 0.2975 = 0.3$ is assumed
- The energy requirement for additional, on-board systems like avionics, flight controls and de-icing is assumed to be $2000W$ on average.

8.3. Approximation of aerodynamic characteristics

As the simulation requires the aerodynamic parameters of c_{w_0}, c_{w_i} as well as c_{a_α}, assumptions about these parameters have to be made before the simulation. As the aircraft is expected to feature similar aerodynamic characteristics as a glider aircraft, as by requiring high aerodynamic efficiency, assumptions are possible.
Data from a CFD-simulation of the Standard-Cirrus-glider was used as a basis of the simulation [19]:

Coefficient	Value
c_{a_α}	5.9
$c_{w_i,\alpha}$	0.018
c_{w_0}	0.2
α_{stall}	$10°$

TAB 6. Aerodynamic coefficients used for the simulation

9. SELECTION OF A PRELIMINARY AIRCRAFT CONFIGURATION

The following approach is applied to iteratively search for the ideal aircraft configuration:

1) Making extensive use of assumptions as well as typical parameters obtained from literature, a first iteration is defined. The aircraft configuration is judged on the basis of the flight profile simulation results
2) As the general physical aircraft parameters have been narrowed down, like overall mass and therefore size, wing area, required engine power including the number of engines, a CAD model of the first iteration configuration is constructed. All equipment is positioned within the fuselage and a wing as well as a tail is designed for the configuration
3) The aerodynamic performance of the first iteration is analysed by means for a CFD simulation. The following outcomes and actions are possible:
   - The aerodynamic performance is roughly equal to the assumed values for the first iteration.
     No further action required, the first iteration is accepted as the baseline configuration
   - The aerodynamic performance is worse than the assumed values for iteration 1. Further action is required, for example:
     - Designing a new aircraft configuration using the acquired aerodynamic parameters from the CFD simulation. If the structural layout of iteration 2 is different to iteration 1, a second CFD simulation is required to confirm the aerodynamic performance
     - The airframe CAD model can be modified in order to achieve the aerodynamic performance. Additional CFD simulations are necessary to confirm the aerodynamic performance
   - The achieved aerodynamic performance is better than initially assumed. In this case, margins can be increased, fuel load can be decreased, structural mass can be increased, or more aggressive flight profiles are possible. As long as the airframe is not altered and the only changes concern mass and the distribution of mass among different aircraft systems, no further CFD simulations are necessary

10. CFD ANALYSIS OF THE AIRFRAME, ITERATION 1

After tweaking the parameters of the flight profile simulation, an acceptable aircraft configuration was found. On this basis, an airframe is designed and tested via a CFD-Simulation.

Of particular interest are the the terms c_{w_0}, $c_{w_i} = \frac{\partial c_w}{\partial \alpha}$ and $c_{A_\alpha} = \frac{\partial c_A}{\partial \alpha}$. It is assumed that c_{w_i} and c_{A_α} share a linear relationship against the angle of attack.
Siemens Star-CCM was used to both mesh the geometry and conduct the flow analysis. The mesh and physics setup was validated by measuring the drag coefficients of spheres, which are very accurately known for different Reynolds numbers.

Note: The air intake of the motor as well as the propeller blades will not be modeled. The rationale for this is the following:
The air intake is sized so that when flying at the highest expected velocity, it delivers exactly the amount of air required for the engine to burn the required fuel. Therefore, the inlet pressure is equal to the total pressure of the flow and little drag is created.
The propeller on the other hand accelerates the airflow passing through it. Instead of drag, it creates thrust. Although the accelerated flow in front of the propeller is disregarded in the simulation, this is deemed acceptable.

10.1. Results, preliminary aircraft design

By simulating attack angles between $-9°$ and $9°$, the following relationships between α and c_w as well as c_{A_α} have been recorded:

AoA	C_w	C_a	L/D
-5	0.0337	-0.09	-2.67
-3	0.0258	0.141	5.5
-1	0.0226	0.337	14.9
1	0.0215	0.608	28.3
3	0.0249	0.865	34.7
5	0.0728	1.914	26.3
6	0.036	1.154	32.1
7	0.0431	1.282	29.7
9	0.0588	1.48	25.2

TAB 7. Aerodynamic Performance

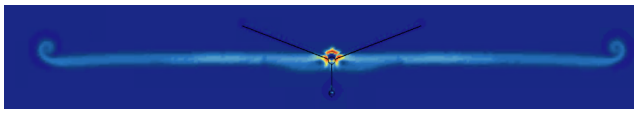

FIGURE 15. Turbulence viscosity ratio, wing tubulence in cruise flight

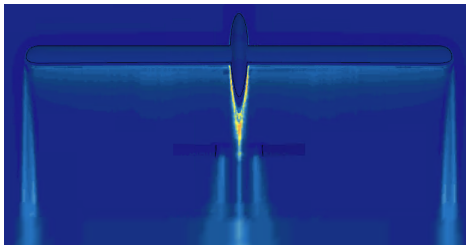

FIGURE 16. Turbulence viscosity ratio, entire aircraft, cruise flight

From the following graphs, it becomes apparent that an aerodynamic stall occurs around and angle of attack of $5°$ degrees. C_a is approximated via a linear regression between angle of attacks of $-5°$ and $4°$. C_w is approximated via a function with the absolute value of α as the variable. The approximations will be considered valid for an angle of attack of $5°$. The simulated data as well as the approximations are shown in the following diagram:

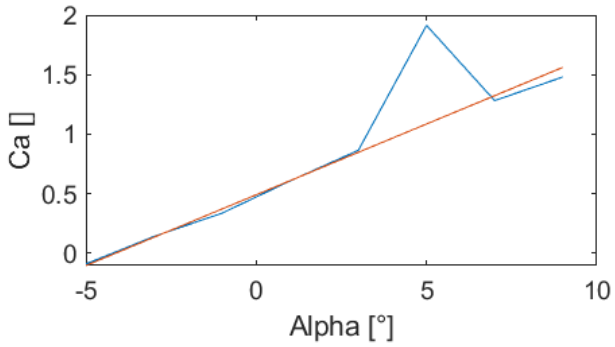

FIGURE 17. Coefficient of lift

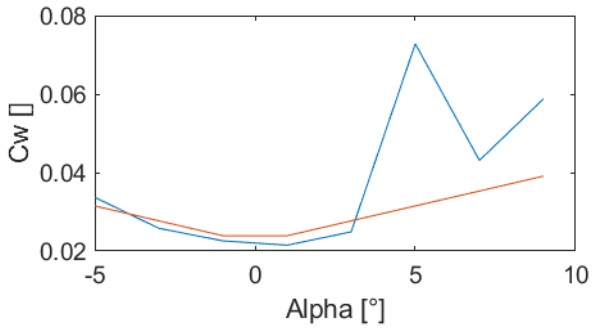

FIGURE 18. Coefficient of drag

The used approximations:

$$C_{a_\alpha} \approx 0.491 + \alpha \cdot 0.1189 \tag{10}$$

$$C_{w_\alpha} \approx 0.022 + |\alpha| \cdot 0.0019 \tag{11}$$

The aerodynamic performance of the airframe concept exceeds the assumed parameters of the first simulation. Therefore, the airframe geometry itself is not changed, but margins are to be increased.

11. SELECTION OF A BASELINE AIRCRAFT CONFIGURATION

11.1. Aircraft configuration, final configuration

After implementing the new, more favourable aerodynamic characteristics in the flight profile simulation, the following aircraft configuration was selected:

Parameter	Value
Structural mass m_{struct}	$550kg$
Fuel mass at takeoff m_{fuel}	$400kg$
Wing area A	$20m^2$
Takeoff / landing elevation	$0m$
Operational altitude	$18000m$
End of ascent	$4500s$ $(10000s)$ (2,8 hours)
Start of descent	$172800s$ (2 d)
Touchdown	$180000s$ (2 d, 2 h)
Takeoff-velocity	$30\frac{m}{s}$
Landing Velocity	$20\frac{m}{s}$
Velocity at arrival at $18000m$	$93\frac{m}{s}$
Velocity, start of descent	$74\frac{m}{s}$
Remaining fuel on landing	$15kg$
Propulsion efficiency	0.28
Peak power	$72000W$
Maximum angle of attack	$3.8°$
Wing relative fuselage angle	$4°$

TAB 8. Single-value results of the selected flight-profile simulation

The most notable changes are an increase in structural mass, a decrease in fuel load as well as a reduction in total propulsion system efficiency to $\eta = 0.28$, to make a more conservative estimate about the development of piston engines. At a propeller efficiency of $\eta_{prop} = 0.85$, the piston engine is only required to reach $\eta = 0.33$. Overall, the selected aircraft configuration offers higher margins than the preliminary design.

11.2. Time-dependant flight parameters

Simulating the modified flight profile as described in table 8, the following flight parameters have been simulated. The yellow and the purple '*' mark the beginning and end of the dash. The red '+' marks two days of elpased time. The green 'o' marks the point of fuel exhaustion:

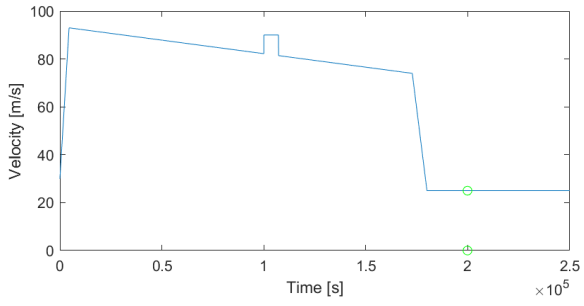

FIGURE 19. Velocity profile

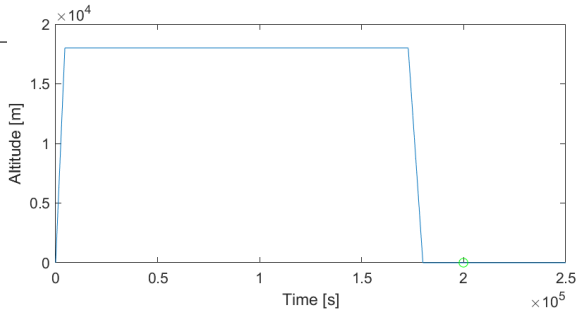

FIGURE 20. Altitude profile

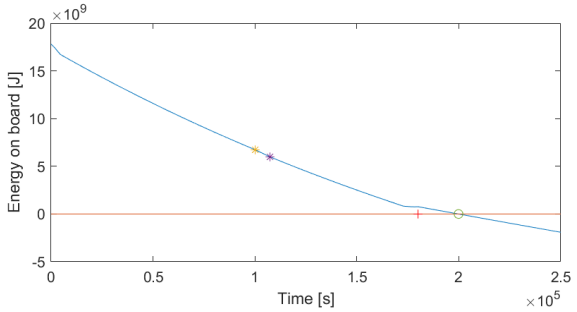

FIGURE 21. Energy on board the aircraft

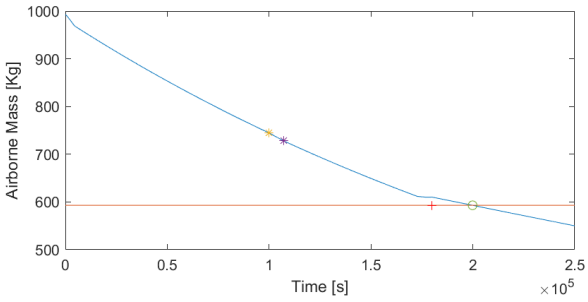

FIGURE 22. Total airborne mass

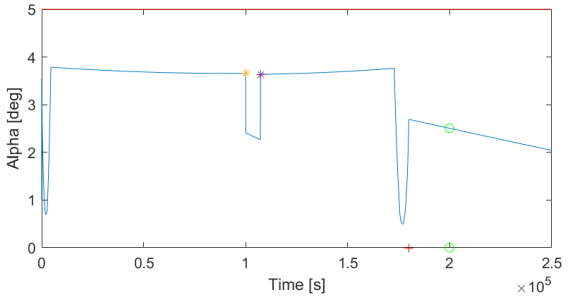

FIGURE 23. Angle of attack

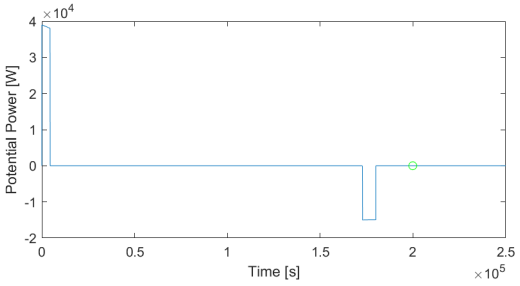

FIGURE 24. Power due to altitude changes

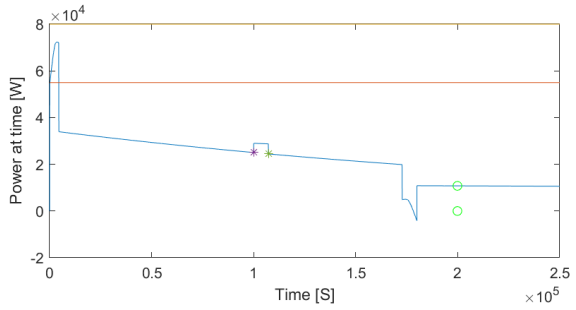

FIGURE 25. Engine Power. Max power and max power for good efficiency are marked by the lines

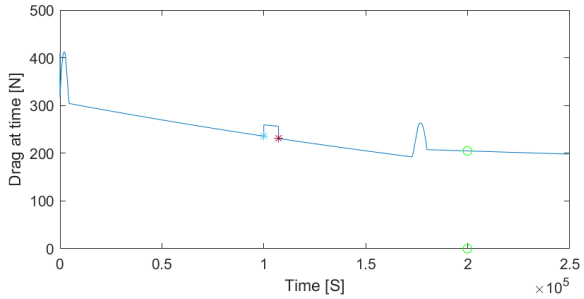

FIGURE 26. Drag

11.3. Margins

- The aircraft lands with $15kg$ of fuel remaining, allowing for 7.51 hours of holding flight at sea level
- Due to the superior aerodynamic performance, the engine power is lower during most flight states, compared to the preliminary aircraft concept
- The aircraft requires $100kg$ less fuel and carries an additional $50Kg$ of structural mass, to increase robustness
- From a performance standpoint, the aircraft is able to climb to $18000m$ in $4500s$, but for thermal reasons, the minimal time to $18000m$ is $10000s$

11.4. Energy characteristics of the dash into scenario 2

As shown in chapter 4.2.2, the dash requires a TAS of $90\frac{m}{s}$. Right until $30000s$ into the simulated flight profile, the base aircraft velocity is higher than the dash velocity. Only after 30000 seconds is the dash velocity higher than the velocity required by the flight profile. The longest possible dash lasts for two hours.
To find the time at which the most energy-demanding dash occurs, two factors need to be taken into account:

- A heavier aircraft requires more energy during the dash, since it needs to be flown at a higher angle of attack, increasing drag
- The later the dash occurs, the larger the energy overhead becomes in contrast to the undisturbed flight profile. While the aircraft, at $90000s$ and flying at $80\frac{m}{s}$ only needs to increase it's speed by an additional $10\frac{m}{s}$ to reach the required dash velocity, the same aircraft, just prior to descent, needs to speed up by an additional $20\frac{m}{s}$ to reach $90\frac{m}{s}$, increasing additional energy demand.

12. STRUCTURAL LAYOUT, BASELINE-CONFIGURATION

12.1. Fuselage

The fuselage was created by using the contour of the symmetric airfoil *s1048-il*. The airfoil is selected for it's relatively low drag coefficient, while offering an extended bulge, which provides sufficient room to accommodate the payload as well as other aircraft hardware. The tail end has been modified, so a propeller hub with a diameter of $200mm$ can be attached.
The length of the fuselage has been selected as $7500mm$ as by the aerodynamic characteristics of the tail surfaces. The largest radius of the fuselage is $520mm$. The upper shell is to be detached above the payload and the engine, to make maintenance easier.

12.2. Wing

The wing is one of the key aspects of an aircraft and greatly defines the flight performances and characteristics. First the key parameters of the wing in cruise conditions at $18km$ altitude need to be determined. High aspect ratio wings are very efficient but generate large wingspans. The aircrafts wing should be transportable in a standard $40t$ truck, so the wingspan needs to be smaller than 12 meters, including transportation stands. Also, the aircraft needs to be able to take and land from small and narrow airfields. So, a balance between efficiency and practicality needed to be found. An aspect ratio of $AR = 15$ is selected. For cheap manufacturing purposes, a non-tapered wing is chosen. Also, the wing will have no sweep, because it is not necessary for the aircraft speeds in the low Mach numbers. Also, it is important to note, that a good lift to drag ratio is desirable. The Wing reference area $S_{ref} = 20m^2$ is obtained from the flight envelope program. Because of the rectangular wing. the following formulas can be used to detemine the wingspan b, the mean-aerodynamic chord MAC. Because of the non tapered wing, the MAC as well as the wing root cord and the wing tip cord are the same.

$$b = \sqrt{S_{ref} \cdot AR} = 17.3205m \tag{12}$$

$$MAC = \frac{b}{AR} = 1.1547m \tag{13}$$

The aim of the flight profile is to cruise at the smallest drag possible. So instead of the commonly used method of constant speed and variable angle of attack, the aircraft flies at a constant angle of attack and varies the speed. The airfoil *NASA NLF1015* offers superb aerodynamic performance, albeit at a low stall angle. originally developed for a NASA research aircraft [20] as described in table 9, it is chosen for the *Sentinel* aircraft.
The aircraft has a similar size and operating parameters compared to our aircraft, which led to the decision to

Aircraft characteristic	Value
Gross weight	$2000kg$
Empty weight	$1000kg$
Payload	$150 - 200kg$
Operational altitude	$20000m$
Endurance	$90h$
Range	$32000km$

TAB 9. Description of NASA research aircraft [20]

choose this air foil. To determine the correct airfoil parameters the Reynolds number is needed:

$$Re = \frac{\rho \cdot v_c \cdot MAC}{\eta} = 9.1854 \cdot 10^5 \approx 1 \cdot 10^6 \tag{14}$$

Out of the graphs for the airfoil at a $Re = 1 \cdot 10^6$ the main characteristics are:

Airfoil characteristic	Value
Zero-Lift Drag Coefficient	$C_{d0} = 0.0075$
Zero-Lift angle	$\alpha_0 = -6.5°$
lift curve slope	$\frac{\delta C_L}{\delta \alpha} = 2 \cdot \pi \frac{1}{rad}$
Max. Lift Coefficient	$C_{L_{max}} = 1.5$
Lift to Drag Ratio	$L_{D_{max}} = 167.7$ at $\alpha = 5°$
Moment Coefficient	$C_{m_af} = -0.19$ at $\alpha = 5°$
Max. Thinkness to Cord	$t_{MAC_{wing}} = 0.15$

TAB 10. Airfoil Characteristics [21]

Wings are most efficient with an elliptical Lift distribution over the wingspan. To achieve this a, slight modification the MATLAB script of [22] is used to find a well-suited wing twist. With a wing setting angle of 5° and a wing twist angle of -2°, a suitable elliptic lift distribution is achieved. As shown in picture 27, it is not a perfect match so an Oswald factor of e = 0.9 is assumed.

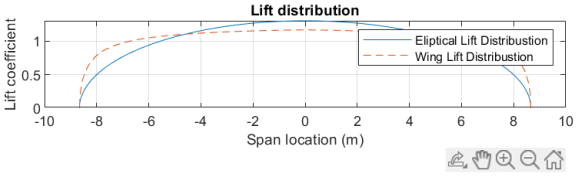

FIGURE 27. Lift distribution

The wing, as it is designed now, might be unsuitable for landings. The landing speed is determined by the following wing equation:

$$V_{land} = 1.2 \cdot \sqrt{\left(\frac{2 \cdot W_{land}}{\rho_0 \cdot C_{L_{max}} \cdot S_{ref}}\right)} \approx 20 \frac{m}{s} \tag{15}$$

This landing speed is really good for conventional aircraft. But our requirement for short take-offs and landings can be improved further by adding a split flap. It will be 60% of the wingspan and 20% of the aircraft's MAC and deployed with $20°$ deployment angle. This results in the lift distribution shown in graph 28.

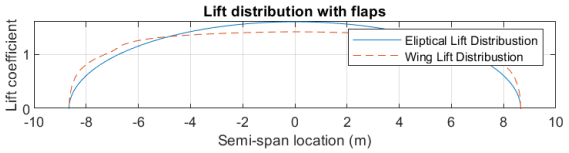

FIGURE 28. Lift distribution with flaps

This flap is chosen because it is cheap and more importantly generates more drag. The aircraft will have a great Lift-to-Drag ratio, but for landing a smaller Lift-to-Drag ratio is better to avoid overshooting the runway. For this reason, the aircraft will land using the stable and high drag slip landing. Lastly, because the aircraft is fitted with independently controllable ailerons. these can be used in a similar manner to spoilers. They can be both angled up to decrease the lift at the wingtips. This feature makes special spoilers unnecessary although this use at the wingtips is less effective than at the wing root, due to the lift distribution.
$370Kg$ of the total fuel load of $400Kg$ is to be stored in the wings, directly above the center of mass. As close to half of the aircraft's takeoff-weight is fuel, a significant shift of the cg is to be avoided. The remaining $30Kg$ of fuel will be stored in a trim tank to more accurately control the center of mass (CoM) during flight.

12.3. Tail surfaces

For the Tail a Y-Tail configuration is chosen. This is to protect the propeller at the back of the aircraft from striking the ground on take-off and landings. For the length between tail and wing a value of $l_{rear} = 3.6$ is chosen. For the vertical tail a volume of $V_V = 0.02$ is chosen as well as a horizontal tail volume $V_H = 0.5$. With the following equations the vertical Tail Surface S_V and the Horizontal Tail Surface S_H are calculated.

$$S_V = \frac{b \cdot S_{ref} \cdot V_V}{l_{rear}} \tag{16}$$

$$S_H = \frac{MAC \cdot S_{ref} \cdot V_H}{l_{rear}} \tag{17}$$

The Y-tail needs to be designed, so the 3 tail surfaces accumulate the desired surface in the horizontal and vertical plain. The symmetrical air foil NACA 0008 is used. It provides very low C_{D_0} while also having a usable thickness for the structural parts of the Tail.

12.4. Propeller

The parameters for the propeller were designed on the basis of the flight envelopes and various flight situations with quantities like thrust, airspeed, density, torque of the shaft and the number of revolutions. To determine the diameter of the propeller formulas from the book "Handbuch der Luftfahrzeugtechnik"by Rossow and Horst [23] were used. The approach was the following: certain quantities were known from the

envelopes and the data sheet of the engine. It was also known what effiency the propeller needed to have in order to generate sufficient thrust. Using the following formula:

$$\eta = \frac{c_f}{c_p} \cdot J \tag{18}$$

with C_f being the thrust coefficient and C_p being:

$$C_p = 2 \cdot \pi \cdot C_m \tag{19}$$

with C_m being the torque coefficient and J the Level of progress [23]

All the coefficients above are dependent on the diameter. To determine them, the diameter is being estimated with the given quantities until the aspired efficiency is being reached. To begin with the estimation, a flight situation is being chosen for the quantities in the coefficient formulas. The situation that was chosen is the moment, were the plane needs the max. continuous power. In this case :

Parameter	Value
Thrust	$511N$
Speed	$90\frac{m}{s}$
Revolutions per Second	$81,66$
Density	$0.364\frac{kg}{m^3}$
Estimated power	$52kW$

TAB 11. Parameters for propeller calculation

From the estimated power that is needed the number of revolutions and the torque can be taken from the manual of the engine. In this case, $52KW$ is about 70% of the max. continous power of the engine. According to the manual, this corresponds to roughly $4900rpm(81,66rps)$ and a torque of $102,5Nm$.Put into the equations above with the diameter of $1.07m$ the coefficients are:

Coefficient	Value
C_f	0.16
C_m	0.03
J	1.03

TAB 12. Propeller coefficients

The efficiency for this case is $\eta = 0.87$. On average 0.85 The propeller will have two blades, due to the fact that a two bladed propeller has a lower mass in comparison to a three bladed propeller. Furthermore, a two bladed configuration offers lower drag in comparison to three blades. Additionally the maintenance and inspection of the two blade variant is easier [23].

12.5. Landing Gear

The exist two suitable options for the landing gear configuration. The first one being a standard Tricycle design and the second one being a Tail dragger design. Both designs shall be able to start and land on short grass strips. Also, both have some advantages or disadvantages over the over design.

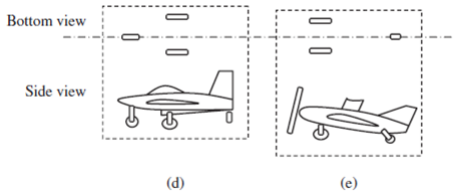

FIGURE 29. Tricycle gear (d) and tail dragger gear (e) [22]

The Tricycle design has one nose gear far from the CoM with $10\% - 20\%$ load and two main Gears close to the cg that carry $80\% - 90\%$ load. One advantage is that the fuselage will be level. Also, this configuration is more stable on the ground, making taxiing easier and enables larger crab angles during crosswind landing. One disadvantage is that the fuselage can tilt back if improperly loaded. Also, the drag is increased during landing and take-off. The tricycle gear is heavier than the taildragger. The tail dragger design uses two main Wheels just in front of the CoM carrying $80\tilde{}90\%$ of the load and a small wheel at the back of the aircraft carrying $10\tilde{}20\%$ of the load. A skid can be used at the back or make the back wheel retractable to decrease drag in flight. The Aircraft's fuselage is often not level due to the smaller back wheel. The angle increases drag at take-off and increases the take off run. Another problem of this design is the natural instability on the ground [22] and requires constant input to keep the aircraft under control.
The decision was made to use a taildragger because it is lighter. The idea is to put a wheel on top of the ruder of the vertical part of the tail, that is pointing downwards. This reduces drag and weight and decreases the angel on the ground. The problem of an increased take off run can be reduced. The instability of this design are controllable because the aircraft is primarily controlled by a computer. Also, every gear is equipped with one wheel to decrease weight and increase drag for landing. Another effect is that the wheels need to be larger than for example a 2-wheel configuration. A larger diameter makes it easier to skip over larger rocks and other debris on a small grass strip. The landing gear shell retractable to reduce drag. This comes at the expanse of higher manufacturing and maintenance cost. Also, it will be heavier than non-retractable landing gears. It will take up space in the fuselage, that could be used differently. The benefits of the design outweigh the disadvantages. The main landing gear will be mounted at the side of the fuselage.

13. MASS OF COMPONENTS

13.1. Comparison of mass ratios

The Maximum Take Off Weight is $993kg$. This is divided into $400kg$ of fuel mass, $550kg$ of empty weight and $43kg$ of payload. This results in the following mass ratios:

(20) $$\frac{m_e}{m_{mtow}} = 0.54$$

(21) $$\frac{m_f}{m_{mtow}} = 0.40$$

(22) $$\frac{m_p}{m_{mtow}} = 0.06$$

In the table below, values from the MQ-1/RQ-1 Predator and RQ-4A Global Hawk are presented, both of which possess similar ratios, thereby demonstrating that the aircraft exhibits realistic force ratios:

	MQ-1 Predator	RQ-4A GH
MTOW [kg]	11612	1020
Fuel Mass [kg]	4173	513
Payload [kg]	6577	302
Empty Weight [kg]	907	204
m_e/m_{mtow} [%]	36	50
m_f/m_{mtow}[%]	57	30
m_p/m_{mtow} [%]	8	20

TAB 13. Mass ratios of comparable aircraft [23]

As can be seen, the mass ratios are similar, with the differences being offset by the very low payload.
Comparing the Sentinel wing loading of $49.65\frac{Kg}{m^2}$ with a full tank and $29.65\frac{Kg}{m^2}$ with an empty tank with glider aircraft wing loadings of 20 to $60\frac{Kg}{m^2}$, a realistic range is achieved. [24]

13.2. Component mass estimation

It is necessary to calculate the expected mass of the wing, fuselage, tail, and landing gear for the design of the aircraft and compare it with the maximum available structural mass. All structural components are made of composite materials. All values for the upcoming calculations of component mass estimations can be found in table 14.

Term	Value
Maximum Take Off Weight [kg]	993
Wingspan [m]	17.3205
Wing Semi Chord Sweep Angle [°]	0
Design ultimate load factor	3
Wing Area [m^2]	20
Maximum thickness of wing root chord [m]	0.12
Vertical Tail Area [m^2]	0.706
Horizontal Tail Area [m^2]	3.42
Maximum fuselage Perimeter [mm]	3251.5
Fuselage Length [mm]	7500

TAB 14. Values to calculate component masses

Using these values, according to the Torenbeek method, for aircraft with a maximum takeoff weight of up to $12.500lbs$, a calculated wing mass of $135.7kg$ is obtained. Additionally, according to the Torenbeek method, for an aircraft with a sinking rate below $250kts$, a calculated tail mass of $30.4kg$ is obtained for the entire tail assembly. [22]
The fuselage is estimated using the *Chessna* method for high wing aircraft with a maximum flight speed below $200kts$. This results in a fuselage mass of $133.3kg$ assuming a pilot is on board. However, since the Sentinel is unmanned, the additional payload required for antenna, relay, and radar is converted to an assumed average body weight of $80kg$. Therefore the payload would conservatively account for approximately 0.7 passengers. This results in a fuselage mass of $109.4kg$. [22]
For the landing gear, an estimated mass of 71.5 kg is obtained. This is calculated using the coefficients for calculating landing gear mass according to Torenbeek. For the Sentinel, the coefficients used for the nose landing gear were: $A_{lg} = 9.1$; $B_{lg} = 0.082$; $C_{lg} = 0$ and $D_{lg} = 2.97 \cdot 10^{-6}$.
For the taildragger, the following values are obtained: $A_{lg} = 9.1$; $B_{lg} = 0.082$; $C_{lg} = 0.019$ and $D_{lg} = 0$.
For aircraft with low takeoff weight, the mass of the landing gear is often around 7% of the maximum takeoff weight. For the Sentinel, it is at 7,2%. [25]
Subtracting all these masses from the maximum structural mass, a remaining structural mass of $87.1kg$ is obtained.To reinforce critical structural components, the vertical tail fin is intended to weigh an additional $26.7kg$ in order to support the attached landing gear. The remaining $70.4kg$ of structural mass will be allocated to reinforce the wing.

13.3. Mass balance calculation

Fuel mass is not regarded in the center of mass (CoM) calculation, with the exception of a $30kg$ trim tank. The rationale for this is the following:

- $370kg$ of the total of $400kg$ of fuel will be stored in the wing. It is assumed that the CoM of the fueled wing is at the $\frac{1}{4}$-line of the wing depth. Therefore, since the wing is placed above the CoM of the aircraft, fuel drained from the wing has no influence on the CoM of the aircraft.
- As the aircraft flies with a high angle of attack during most of the flight profile, the fuel remaining in the wing will collect at the rear of the wing, shifting the CoM slightly backwards. To counteract this, a small trim tank of $30kg$ is placed in front of the aircraft CoM and is drained only later in the flight profile to counteract this mass shift

To always ensure a boundary-stable aircraft configuration, the wing will be placed at $3342mm$ aft of the nose. The CoM shifts by a maximum of $10cm$.

Component	Mass	X-Coordinate
Payload		
7 x Relais	$35kg$	$1340mm$
1 x Radar	$5kg$	$600mm$
1 Antenna Relais	$2kg$	2420
1 Antenna GND	$1kg$	2420
Avionics		
3 x Flight Computer	$0.48kg$	$1380mm$
3 x INS system	$13.5kg$	1170
Energy Systems		
3 x Battery	$17.01kg$	$1740mm$
1 x Engine	$70kg$	3650
1 x Propeller	$15kg$	$7070mm$
Fuel systems		
Trim tank full/empty	$30kg$ / $0kg$	$2050mm$
Structure		
Fuselage	$109.4kg$	$3037mm$
Tail	$57.1kg$	$7000mm$
Main Gear	$71.5kg$	$2400mm$
CoG tank full		$3342mm$
CoG tank empty		$3440mm$

TAB 15. Center of gravity calculation, full fuel / emtpy fuel tanks

13.4. Distribution of components

Compared to the preliminary aircraft configuration, the fuselage, wing and tail have remained unchanged, however, some components have been moved. A section view of the fuselage interior is seen in figure 30:

Component	Color
Radar module	Orange
Flight Computers & INS	Dark blue
Broadband relais	Light blue
Batteries	Red
Trim Tank	Green
Antennas	Yellow
Landing gear	Purple
Engine	Gray

TAB 16. Component colors

13.5. Fueling concept

For the storage of fuel, a tank in the fuselage of the aircraft is used, which can hold 30kg of fuel. The remaining 370kg of fuel, which are allocated for the flight, should be accommodated in the wings. With a minimum density of Avgas of $0.73kg/l$, a tank of 506.8 liters will be necessary. Therefore, approximately $0.51m^3$ of tank needs to be accommodated in the wings. Divided between 2 wings, that makes $0.255m^3$ per wing. In order to prevent the weight of the fuel from excessively stressing the wing when on the ground, as much fuel as possible should be placed as close as possible to the fuselage. With a wing cross-sectional area of $0.133m^2$, there is enough margin left with a utilization of $0.08m^2$ for the tank to ensure a stable wing. From the required tank and the cross-sectional area, a length of 3,2m is needed within the wing for the tank.

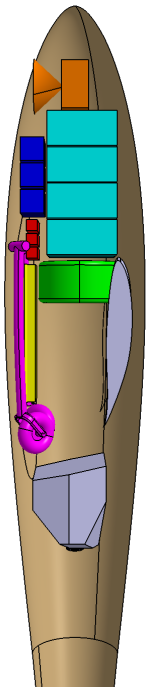

FIGURE 30. Internal distribution of components, flight direction is 'up'

The refueling of the aircraft is done through a simple valve on the top of the wing. There is also a separate valve for tank ventilation located there. The fuel is also easily transferred to the engine through the fuel pump installed in the engine and the higher positioned wing.

To minimize emissions despite the combustion of fuel, it is part of the concept to use synthesized fuel. Through synthesis with renewable energy sources, the aircraft is almost emission-free throughout. This is already possible and is expected to be further developed technologically by 2040 to achieve higher efficiency and lower prices in fuel production. However, in order to enable global implementation, it must be available everywhere. Forecasts predict the growing use of Sustainable Aviation Fuel, aiming to achieve 20% of Aviation Fuel Consumption through Sustainable Aviation Fuel by 2040. Therefore, it can be assumed that synthetic fuels, including AvGas, will be used worldwide and thus be available everywhere. [26]

14. AIRCRAFT PERFORMANCE

Figure 31 shows the drag polars for horizontal flight at 18km. The pink dots are the stall speed. The black dots are at the speed for lowest drag. The weights of the aircraft are varied from MTOW to empty weight.

Figure 32 shows the curve radius of a turn with a min curve radius with $545m$ at a velocity of $96\frac{m}{s}$.

Figure 33 shows the turn rates with a min turn time of $5.67s/rad$ at a velocity of $96\frac{m}{s}$. This results in a min time of $34s$ for a full circle.

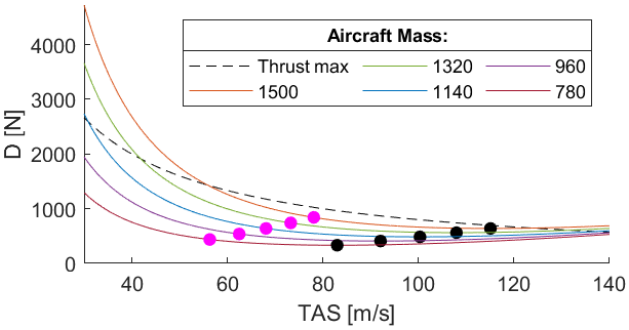

FIGURE 31. Drag horizontal flight at 18km

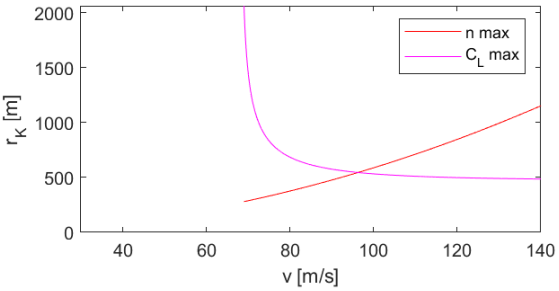

FIGURE 32. min curve radius

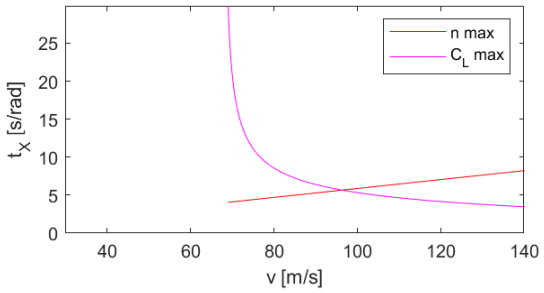

FIGURE 33. max turn rate

The figure 34 shows the pull up radius at 18km height while 35 shows the same at sea level. The pink dots are the stall speed.

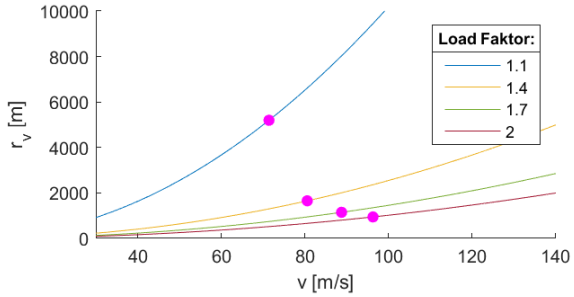

FIGURE 34. Pull-Ups at 18 km

The figure 36 shows the loads in 18km heights. The pink lines show the stall speed at certain loads. The orange lines represent the limit load and the red lines the ultimate loads. The black dotted lines representing the gust loads with FAR 25 default gust speeds. The maneuvering speed is $96\frac{m}{s}$.

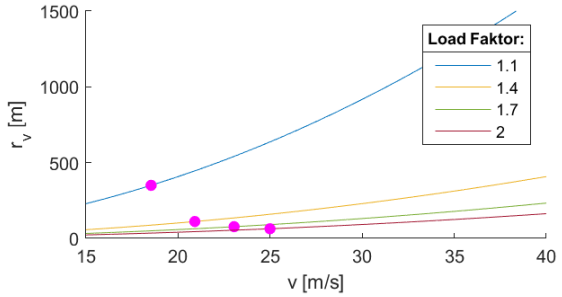

FIGURE 35. Pull-Ups at 0km

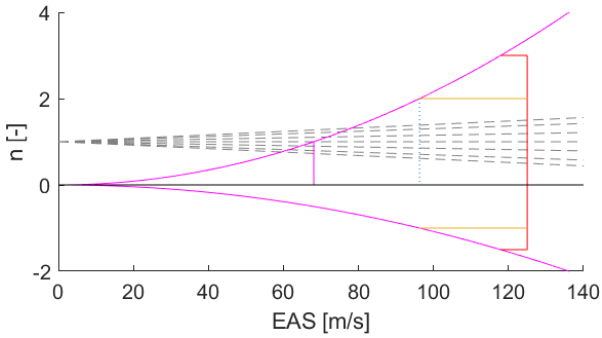

FIGURE 36. v-n Diagram in 18 km

15. THERMAL MANAGEMENT

At an altitude of $18000m$, the ambient temperature is $216.5K$, as by the standard atmosphere [27]. It has to be assured that sensitive hardware isn't rendered inoperable by low temperatures. At the same time, the waste heat of the engine must be dissipated to avoid overheating the aircraft.

15.1. Heat sources

Two main sources of heat can be identified on board the aircraft:

- The engine, with $\eta \approx 0.35$, emits 70% of the total engine power as heat energy. Of the total engine power, roughly 20% to 40% is lost through the exhaust. Due to the EIS date, it is deemed acceptable to assume a high value for the exhaust energy fraction, in this case, 35% will be used. With 35% of total engine power being transmitted as mechanical power, a further $\eta_f = 30\%$ is emitted by the engine into the fuselage.
- The payload as well as other electronic equipment on board emits waste heat, since it doesn't operate at 100% efficiency. As there is no information on the efficiency of the payload given, a base efficiency of $\eta = 0.8$ is assumed for all electric systems. With the payload drawing $3950W$ and $2000W$ being allocated for other on board systems, $1190W$ is emitted into the fuselage.

Heat is dissipated through the airframe to the surrounding atmosphere by conduction between the fuselage skin and the surrounding air.

To calculate the heat transfer coefficient, it is assumed that heat is dissipated to the boundary layer, where it is transported away by convection. However, the waste heat doesn't need to be transported through the entire boundary layer, since the velocity inside the boundary layer

starts to increase, the greater the distance to the static layer.
Therefore, it is assumed that the waste heat needs to be only transported through half the boundary layer for full dissipation.
Furthermore, it is assumed that heat movement inside the fuselage is instantaneous, e.g. heat from the engine is spread equally throughout the entire fuselage.
The coefficient of heat transfer is then calculated as follows, with α_f being the coefficient of heat transfer through the fuselage skin and α_b being the coefficient of heat transfer through the boundary layer [28]:

$$\alpha_{tot} = \frac{1}{\frac{1}{\alpha_f} + \frac{1}{\alpha_b}} \tag{23}$$

The heat transfer coefficient is calculated from the thermal conductivity of a material and the layer thickness. There is $109Kg$ of structural mass available for the fuselage. Furthermore, it is assumed that 50% of that mass is reserved for stringers, internal structures and other parts that don't share a contact surface with the air stream.

15.1.1. Fuselage heat transfer coefficient

To estimate a wall thickness, the aircraft fuselage of the CAD model is thickened until the mass is $109kg \cdot 0.5 = 54.5kg$. The resulting wall thickness t_f is $3mm$. The thermal conductivity of carbon fibre is estimated at $15\frac{W}{m \cdot K}$ [29]. Therefore, the total heat transfer coefficient of the carbon fibre skin is [30]:

$$\alpha = \frac{\lambda}{t} \tag{24}$$

$$\alpha_f = \frac{15\frac{W}{m \cdot K}}{0.006m} = 2500\frac{W}{m^2 \cdot K} \tag{25}$$

15.1.2. Boundary layer heat transfer coefficient

The thickness of the boundary layer is dependant on the x-coordinate of the flow. The thickness of the boundary layer increases, as the flow travels further down the length of the fuselage.
The Reynolds-number as a function of the x-coordinate of the fuselage is calculated as follows, using $\rho = 0.12$, $v = 90\frac{m}{s}$ and the dynamic viscosity $\eta_v = 1.422 \cdot 10^{-5}\frac{N \cdot s}{m^2}$ [27]

$$Re = \frac{v \cdot \rho \cdot x}{\eta_v} \tag{26}$$

To approximate the boundary layer thickness as a function of the Reynolds number, formula 27 is used [31]. Although the formula only applies for a planar surface, it is deemed to be sufficient to calculate a rough value of the boundary layer thickness. The factor 2 in the denominator is included to account for only half of the boundary layer thickness δ:

$$\delta = 5 \cdot \frac{x}{2 \cdot \sqrt{Re(x)}} \tag{27}$$

As the coefficient of heat transfer can be calculated from the thermal conductivity using the thickness of the transmission layer, α_{tot} can be calculated as a function of x, using the thermal conjunctivitis $\lambda_a = 0.02 \cdot \frac{W}{m \cdot K}$ and $\lambda_f = 15 \cdot \frac{W}{m \cdot K}$ of air and the fuselage:

$$\alpha_{tot} = \frac{1}{\frac{t_f}{\lambda_f} + \frac{5 \cdot \frac{x}{2 \cdot \sqrt{Re(x)}}}{\lambda_b}} \tag{28}$$

To solve for the equilibrium temperature in the fuselage for $\lim_{t \to \infty} T(t)$ for a given engine power, the following equation with A being the surface area of the fuselage is rearranged with $\dot{Q} = \eta_f \cdot P_{eng}$:

$$\dot{Q} = [T_f - T_a] \cdot \alpha_{tot}(x) \cdot A(x) \tag{29}$$

$$T_f = \frac{\dot{Q}}{\alpha(x) \cdot A(x)} + T_a \tag{30}$$

The expression 30 can be rewritten as equation 31 with l_f being the fuselage length.

The radius function of the fuselage has been interpolated as a polynomial of the 7^{th} degree, $r(x) = \sum a_n x^n$, using the following coefficients:

Coefficient a_n	**Value**
a_7	0.0000353493
a_6	-0.000970114
a_5	0.0109611
a_4	-0.0665929
a_3	0.242699
a_2	-0.576517
a_1	0.827385
a_0	0

TAB 17. Interpolation coefficients

Therefore, the equilibrium temperature T_f can be expressed via the equation 31.

$$T_f = \frac{\dot{Q}}{2 \cdot \pi \cdot \int_0^{l_f} \alpha_{tot}(x) \cdot r_f(x)\, dx + T_a} \tag{31}$$

With integral 32 being used to calculate the total thermal emission coefficient of the entire fuselage:

$$a_{tot}(x) \cdot A(x) = 2 \cdot \pi \cdot \int_0^{l_f} \alpha_{tot}(x) \cdot r_f(x)\, dx \tag{32}$$

Evaluating the integral 32 with:

- $\rho = 0.1205 \frac{kg}{m^3}$
- $t_f = 0.003m$
- $\lambda_f = 15 \frac{W}{m \cdot K}$
- $\lambda_b = 0.02 \frac{W}{m \cdot K}$
- $v = 90 \frac{m}{s}$
- $\eta_v = 1.224 \cdot 10^{-5} \frac{N \cdot s}{m^2}$

Results:

$$a_{tot}(x) \cdot A(x) = 111.2 \quad \frac{W}{K} \tag{33}$$

Therefore, the fuselage temperature for $\lim_{t \to \infty} T(t)$ and any given engine power is given as:

$$\lim_{t \to \infty} T_f(t) \quad T_f = \frac{\dot{Q}}{111.2 \frac{W}{K}} + 216.5K \tag{34}$$

15.2. Thermal flight profile analysis

Plotting equation 34 over the simulated flight profile, while assuming that 30% of the total engine power plus an additional $1190W$ is transmitted into the fuselage, results in the following blue temperature graph with an ambient temperature of $261.5K$. The purple line marks a temperature of $60°C$, the red line a temperature of $0°C$, being selected as the upper and lower temperature limits to avoid problems with icing and overheating of equipment. The yellow graph shows the difference between the ambient temperature and the fuselage temperature:

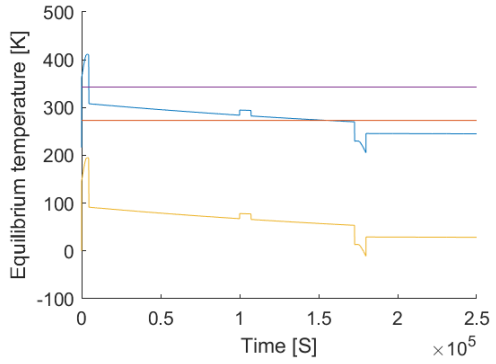

FIGURE 37. Equilibrium temperature profile in the fuselage

As is evident, the maximum allowable temperature is exceeded during climb to cruise altitude. To mitigate this, a flight profile is simulated with a time of $10000s$ to reach $18000m$. In this case, the maximum temperature is $78°C$. Although higher than the maximum acceptable temperature, the engine is not held at this power setting for extended periods of time. The max temperature is exceeded for $2800s$. Furthermore, the plot only shows the temperature for $\lim_{t \to \infty} T(t)$. Since the critical flight state only lasts for a fraction of an hour, $78°$ is likely not reached.
During the last 14000 seconds of flight at $18000m$, the minimum temperature is not met, with the lowest fuselage temperature simulated at $-3°C$. However, this temperature is not deemed critical as well, since only little excess power is required to keep the electronics sufficiently warm. However, the $1190W$ that was originally budgeted for electric equipment waste heat, is directly generated at the equipment itself, so in reality, temperature is expected to be slightly higher and equipment under-cooling is avoided.

15.2.1. Wing tank thermal management

Fuel thermal management is not expected to be an issue, as the freezing point of AvGas lays at around $-100°$, which is still lower than the ambient temperature at $18000m$. Additional heating is not required.

15.2.2. Descent thermal management

As the engine power is greatly decreased during descent, the equilibrium temperature inside the fuselage starts to drop. Since the ambient air temperature starts to increase again as the aircraft looses altitude, the delta of the fuselage temperature in comparison to the ambient temperature is considered. The delta reaches values as low as $13K$ at idle power. Therefore, heating of the electronic equipment is necessary.
Since the fuel doesn't require additional heating as explained in chapter 15.2.1 and the payload is not expected to be operated at full power during descent, only the avionics and flight computers need heating. This is to be realized using electric heating elements. The power is to be allocated from the the payload, offering $3950W$ of heating power. This is deemed to be sufficient to heat components inside the fuselage, without direct contact to the aircraft's skin.

16. WEATHER RESISTANCE

For analysing the weather resistance the gusts in vertical and horizontal direction are required. For the calculation of the horizontal gust speed u_g and the vertical gust speed w_g the source [23] and the following parameters are used.

- $m_{cruise/max} = 793kg$
- $m_{landing} = 593kg$
- $m_{mtow} = 993kg$
- $V_{cruise} = 74 \frac{m}{s}$
- $V_{max} = 90 \frac{m}{s}$
- $V_{landing} = 20 \frac{m}{s}$
- $V_{takeoff} = 30 \frac{m}{s}$
- C_A and $\frac{dC_A}{d\alpha}$ as in chapter 10
- $n_{limitload} = 2$
- $n_{ultimateload} = 3$
- $S = 20m^2$
- $l_m = 1.154m$
- $g = 9.81ms^2$
- $\rho_{18000m} = 0.1205 \frac{Kg}{m^3}$
- $\rho_{0m} = 1.225 \frac{Kg}{m^3}$

Those are resulting in the gust speeds in table 18 and 19:

	limit load	ultimate load
takeoff	$4.77\frac{m}{s}$	$9.54\frac{m}{s}$
cruise	$92.19\frac{m}{s}$	$184.38\frac{m}{s}$
max	$75.80\frac{m}{s}$	$151.60\frac{m}{s}$
landing	$4.17\frac{m}{s}$	$8.33\frac{m}{s}$

TAB 18. Horizontal gust speed, while takeoff, cruise and maximum speed and landing

	limit load	ultimate load
takeoff	$5.53\frac{m}{s}$	$11.06\frac{m}{s}$
cruise	$17.03\frac{m}{s}$	$34.06\frac{m}{s}$
max	$14.00\frac{m}{s}$	$28.00\frac{m}{s}$
landing	$8.11\frac{m}{s}$	$16.23\frac{m}{s}$

TAB 19. Vertical gust speed, during takeoff, cruise and maximum speed and landing

Thus it is possible to start and land the airplane with gust speeds of a fresh breeze, according to the *Beaufort scale*. Upon reaching the targeted operational altitude, the aircraft can fly at cruising speed in gust speeds with hurricane speed and at top speed in with the speed of a violent storm.

17. CONTINGENCY SCENARIOS

In this chapter, multiple emergency scenarios are discussed and different solutions and their implementations on board the aircraft are explained.

17.1. Engine failure scenarios

Generally, an engine failure is handled as follows:

1) Switch off the payload ($3950W$ of power saved)
2) Switch avionics, flight computers and aerodynamic controls to battery power
3) If the airfield can be reached via gliding in two hours and with the given altitude: **Attempt airfield landing**
4) If the airfield is out of reach for the given battery charge or altitude: **Conduct an emergency landing**, making use of image analysis using the camera

17.2. Avionics / Computer failures

Both the flight computers as well as the navigation systems are double-redundant, e.g. there are three of each component carried.

17.2.1. Single component failure

If only one component fails, the following procedure is to be implemented:

1) A voting system is to be implemented. In case of a single component failure, the remaining two components should produce the same values for a given flight state. Therefore, the malfunctioning component can be identified
2) After one component has been voted out, the voting scheme can no longer be used for that set of components

17.2.2. Multiple component failure

In case two components of the same type fail, a voting system might not be applied, as all three components are expected to produce different values. The following approach is to be followed:

1) Should the values of two components drop or increase to an erroneous value, such as a sudden drop of air speed or position to zero or to infinity. Furthermore, sudden switches of the sign of number might be an indication of a component failure.
   Should a component produce a value which is very unlikely to occur in the given flight state or is not achievable withing the aircraft performance, the component is to be ignored

17.3. Navigation failures

17.3.1. Loss of primary navigation

As explained on chapter 7, the primary radar guidance system requires a LoS with the operational base, which is lost during a descent below the radar horizon or a technical malfunction. **In case of a loss of LoS, navigation is switched to backup INS navigation**, using the last up-to-date state vector

17.3.2. Loss of primary and backup navigation

During this dangerous and unlikely scenario, the state vector of the aircraft can no longer be updated and the position of the aircraft is lost.
However, the camera on board the aircraft can still be used to identify suitable emergency landing sites, although their location is not known to the aircraft. **Therefore, an emergency landing or a crash into an uninhabited area may still be attempted**, albeit at great risk to humans and infrastructure as well as the aircraft

17.4. Loss of battery capacity

The aircraft carries $17Kg$ of batteries on board, allowing 3 hours of operations of on-board systems at $2000W$. However, 2 hours is deemed sufficient time to make an emergency descent from $18000m$. Therefore, the batteries are designed in a single-redundant way by including three batteries with a mass of $5.7Kg$ each. Using this system, **any single battery can fail while the other two still hold enough energy for 2 hours of operations**.

18. SUMMARY OF KEY TECHNOLOGIES

To allow the aircraft to achieve the specified performance and complete it's mission in an ecological and economical fashion, the following key technologies are paramount:

- Sustainable aviation fuels are widely adopted by the aeronautical industry to enable net zero emission for the Sentinel system. [32]
- Piston engines for light aircraft applications are expected to reach at least 33% efficiency by the EIS date. [33]
- Piston engines are required to exhaust at least 35% of waste heat through the exhaust to avoid overheating the aircraft.
- Inertial navigation systems are required to reach high levels of accuracy, sufficient to fly $500km$ to the vicinity of an airfield.
- Image analysis needs to be able to reliably identify safe landing zones for emergency scenarios. The analysis can be realized by artificial intelligence and image recognition. [34]

Literatur

[1] Deutscher Wetterdienst. *Jetstream (Strahlstrom)*. Deutscher Wetterdienst, N.a.

[2] N.a. *Tupolev Tu-95LAL*. https://en.wikipedia.org/wiki/Tupolev_Tu-95LAL, 2023. Last accessed:09.07.2023.

[3] idealhy.com. *Liquid Hydrogen Outline*. https://www.idealhy.eu/index.php?page=lh2_outline, N.a. Last accessed: 27.01.23.

[4] wikipedia.com. *Energy density*. https://en.wikipedia.org/wiki/Energy_density, 2023. Last accessed: 29.05.23.

[5] N.a. *Verbrenner-Verbot: Ab 2035 keine neuen Diesel und Benziner mehr*. ADAC, 2023.

[6] DR. OMAR MEMON. *The Power Chain Efficiency Of An Electric Aircraft*. simpleflying.com, 2022. Last accessed: 02.06.23.

[7] Dieter Scholz Andreas Johanning. *Propeller Efficiency Calculation in Conceptual Aircraft Design*. HAW Hamburg, 2013.

[8] D.Stolten A.Glüsen, M. Müller. *45% Cell Efficiency in DMFCs via Process Engineering*. Wiley.com, 2020.

[9] Yvonne Gibbs. *NASA Armstrong Fact Sheet: Perseus B Remotely Piloted Aircraft*. Natioanl Aeronautics and Space Agency, 2014. Last accessed:10.07.2023.

[10] N.a. *Operator's Manual for Rotax Engine Type 914 Series*. Rotax Aircraft Engines, 2010.

[11] N.a. *Cobra: Hallenkuller Einsitzer*. https://www.cobratrailer.com/catalog/product_info.php?products_id=37, N.a. Last accessed: 07.07.23.

[12] N.a. *EDRX info*. https://www.edxr.de/info, N.a. Last accessed: 01.07.23.

[13] N.a. *General Atomics MQ-1 Predator*. https://warriorlodge.com/pages/general-atomics-mq-1-predator, N.a. Last accessed: 03.07.23.

[14] N.a. *Stemme AG auf Erfolgskurs: Verkaufsschlager S12G mit Garmin-Glascockpit*. https://www.aerokurier.de/segelflug/stemme-ag-auf-erfolgskurs-verkaufsschlager-s12g-mit-garmin-glascockpit/, N.a. Last accessed:06.07.23.

[15] Braun; Kirchner; Stoll; Kisch. *Kompass Dokumentation*. Projektbericht, 2023.

[16] N.a. *Laseref VI*. Honeywell technical document, 2016.

[17] N.a. *VECTOR-MCC*. VECTOR-MCC, N.a.

[18] Toni Bingelis. *The Fixed Pitch Propeller Dilemma*. EAA Sport Aviation, 1986.

[19] Thomas Henrik Hansen. *Modeling the Performance of the Standard Cirrus Glider using Navier-Stokes CFD*. ResearchGate, 2014.

[20] Dan M. Somers Mark D. Maughmer. *An airfoil designed for a high-altitude, long endurance remotely piloted vehicle*. NASA Langley Research Center, 1987. Last accessed:20.06.2023.

[21] N.a. *Airfoil Tools*. http://airfoiltools.com/airfoil/details?airfoil=nlf1015-il, N.a. Last accessed:04.07.2023.

[22] Daniel P. Raymer. *Aircraft Design: A Conceptual Approach*. American Institute of Aeronautics and Astronautics, 1989. ISBN 0930403517.

[23] Cord-Christian Rossow. *Handbuch der Luftfahrzeugtechnik*. Hanser Verlag, 2014. 978-3-446-42341-1.

[24] wikipedia.com. *Flächenbelastung (Flügel)*. https://de.wikipedia.org/wiki/Fl2021. Last accessed:09.07.2023.

[25] Dieter SCHOLZ. *Aircraft Design*. http://hoou.ProfScholz.de, 2015. Last accessed:09.07.2023.

[26] IEA. *Aviation fuel consumption in the Sustainable Development Scenario, 2025-2040*. https://www.iea.org/data-and-statistics/charts/aviation-fuel-consumption-in-the-sustainable-development-scenario-2025-2040, 2019. Last accessed: 09.07.2023.

[27] N.a. *U.S. Standard Atmosphere vs. Altitude*. https://www.engineeringtoolbox.com/standard-atmosphere-d_604.html, N.a. Last accessed: 08.07.23.

[28] Peter Gerd Fisch. *Thermodynamik in der Luft- und Ruamfahrt*. DHBW Friedrichshafen, 2023. Vorlesungsskript.

[29] Anthony R. Bunsell. *Handbook of Properties of Textile and Technical Fibers*. Elsevier Ltd, 2018. ISBN 978-0-08-101272-7.

[30] Dr. Sebastian Türk. *Aerodynamik I*. DHBW Friedrichshafen, N.a. Vorlesungsskript.

[31] Hermann Schlichting. *Boundary Layer Theory*. McGraw Hill, 1979. N.a.

[32] N.a. *Sustainable Aviation Fuels Guide*. ICAO, 2017. Last accessed: 09.07.2023.

[33] Felix Leach;Richard Stone;Paul Miles;Gautam Kalghatgi. *The scope for improving the efficiency and environmental impact of internal combustion engines*. sciencedirect, 2020.

[34] N.a. *Image Recognition: The Basics and Use Cases (2023 Guide)*. https://viso.ai/computer-vision/image-recognition/, 2023. Last accessed: 09.07.2023.